Kaunas University of Technology

Faculty of Electrical and Electronics Engineering

Machine Learning for Optimal Cerebral Perfusion Pressure Identification in Traumatic Brain Injury Patients

Master's Final Degree Project

Katherine Boere

Project author

Dr. Vytautas Petkus

Supervisor

Kaunas, 2021

Kaunas University of Technology

Faculty of Electrical and Electronics Engineering

Machine Learning for Optimal Cerebral Perfusion Pressure Identification in Traumatic Brain Injury Patients

Master's Final Degree Project

Biomedical Engineering (6211EX002)

Katherine Boere

Project author

Dr. Vytautas Petkus

Supervisor

Monika Butkuvienė

Reviewer

Kaunas, 2021

Kaunas University of Technology

Faculty of Electrical and Electronics Engineering

Katherine Boere

Machine Learning for Optimal Cerebral Perfusion Pressure Identification in Traumatic Brain Injury Patients

Declaration of Academic Integrity

I confirm the following:

1. I have prepared the final degree project independently and honestly without any violations of the copyrights or other rights of others, following the provisions of the Law on Copyrights and Related Rights of the Republic of Lithuania, the Regulations on the Management and Transfer of Intellectual Property of Kaunas University of Technology (hereinafter – University) and the ethical requirements stipulated by the Code of Academic Ethics of the University;

2. All the data and research results provided in the final degree project are correct and obtained legally; none of the parts of this project are plagiarised from any printed or electronic sources; all the quotations and references provided in the text of the final degree project are indicated in the list of references;

3. I have not paid anyone any monetary funds for the final degree project or the parts thereof unless required by the law;

4. I understand that in the case of any discovery of the fact of dishonesty or violation of any rights of others, the academic penalties will be imposed on me under the procedure applied at the University; I will be expelled from the University and my final degree project can be submitted to the Office of the Ombudsperson for Academic Ethics and Procedures in the examination of a possible violation of academic ethics.

Katherine Boere
Confirmed electronically

Boere, Katherine. Machine Learning for Optimal Cerebral Perfusion Pressure Identification in Traumatic Brain Injury Patients. Master's Final Degree Project / Dr. Vytautas Petkus; Health Telematics Institute, Kaunas University of Technology.

Study field and area (study field group): Bioengineering, Engineering Sciences.

Keywords: cerebrovascular autoregulation; critical care; optimal cerebral perfusion pressure; pressure reactivity index; traumatic brain injury; machine learning

Kaunas, 2021. 54 pages.

Summary

Traumatic brain injury (TBI) is a major global health concern that generates a significant burden on society through mortality, disability, socioeconomic losses, and reduced quality of life. In an acute medical setting, timely maintenance of patient-specific optimal cerebral perfusion pressure (CPPopt) is critical for a positive outcome in patients with severe TBI. However, the wide clinical application of CPPopt-based therapy is limited by the nature of slow arterial blood pressure (ABP) and intracranial pressure (ICP) waves. These waves are transient and intermittent, and therefore directly affect the result of calculated CPPopt values. In current practice, ABP and ICP waves must be monitored for at least 4 hours to obtain sufficient data to determine the CPPopt value. This results in delayed CPPopt management therapy, which can adversely affect a patient's treatment when an alarm for critical brain injury events is delayed or missed. The clinical applicability of the method is also limited by artifacts in patient monitoring signals, which deteriorate usable data by 40–50%. The goal of this research was to develop a machine learning (ML) algorithm that classifies patient ICP and ABP data segments as 'informative' or 'non-informative', using only the informative data to subsequently calculate individualized CPPopt values. The study contained a retrospective analysis of multi-modal physiological monitoring data from 84 severe TBI patients between 2013 and 2018. A unique software tool was designed to create a database of distinct informative and non-informative monitoring episodes. Two supervised machine learning models, Support Vector Machine with a Radial Basis Function kernel and Artificial Neural Network, were developed that each learned to classify patient data segments as informative or non-informative. The algorithm's performance was evaluated for accuracy, sensitivity, and specificity using SPSS Statistical Software. The association of CPPopt-related parameters after applying ML algorithms with the patient outcome was determined through regression analysis. The results indicate that the ML algorithm increased classification accuracy by approximately 4.5% in distinguishing informative and non-informative events (77.58% to 82.1%). However, the most distinguished finding from this research is that when informative physiological ABP/ICP changes are present it is possible to detect individualized CPPopt values in a 10 times shorter time window (20–30 minutes) compared to the clinical standard of 4 hours. Further prospective clinical studies are required to add strength and to determine the benefits of the developed ML method.

Boere, Katherine. Mašininio mokymosi taikymas optimalios smegenų perfuzijos slegio vertei identifikuoti galvos smegenų traumą patyrusiems pacientams. Magistro baigiamasis projektas / vadovas dr. Vytautas Petkus; Kauno technologijos universitetas, Sveikatos telematikos mokslo institutas.

Studijų kryptis ir sritis (studijų krypčių grupė): Bioinžinerija, inžinerijos mokslai

Reikšminiai žodžiai: smegenų kraujotakos autoreguliacija, optimalus smegenų perfuzijos slėgis, mašininis mokymas, galvos smegenų trauma, slėgio reaktyvumo indeksas.

Kaunas, 2021. Puslapių sk. p. 54.

Santrauka

Galvos smegenų trauma (GST) yra globali sveikatos problema, susijusi su padidėjusiu visuomenėje mirtingumu, neįgalumu, socialiniais-ekonominiais nuostoliais ir suprastėjusia potrauminio gyvenimo kokybe. Intensyviojoje terapijoje, savalaikis ir individualizuotas GST gydymas paremtas optimalaus smegenų perfuzijos slėgio (OptSPS) palaikymo terapijos taikymu yra svarbus siekiant pagerinti GST pacientų klinikines baigtis. Tačiau šios terapijos klinikinį taikymą riboja tai, kad OptSPS vertės nustatymui yra naudojamos lėtosios arterinio kraujospūdžio (AKS) ir intrakranijinio slėgio (IKS) bangos, kurios yra nepastovios amplitudės, atsitiktinai atsirandančios ir išnykstančios. Nepakankama ir nepastovi šių bangų amplitudė yra pagrindinis veiksnys reikalaujantys ilgo mažiausiai 4 valandų AKS/IKS stebėsenos duomenų kaupimo reikalingo OptSPS vertės nustatymui. Toks vėlavimas neigiamai įtakoja paciento gydymą, kai kritinių smegenų pažeidimų įvykių aliarmas yra uždelsiamas arba praleidžiamas. Šio darbo tikslas yra sukurti mašininio mokymo (MM) algoritmą, kuris leistų GST pacientų AKS ir IKS stebėsenos duomenyse aptikti informatyvius duomenų epizodus iš kurių būtų galima patikimai nustatyti OptSPS vertę bei parinkti paciento gydymui tinkamą gydymo terapiją. Šiai užduočiai spręsti buvo panaudoti 84 sunkią GST patyrusių pacientų multimodalinės stebėsenos duomenų surinkti Lietuvoje klinikinių tyrimų metu 2013-2018 metais. Šių duomenų analizei buvo sukurtas unikali programinė priemonė leidžianti klasifikuoti informacinius ir neinformacinius multimodalinės stebėsenos epizodus bei sudaryti šių duomenų bazę. Informacinių ir neinformacinių multimodalinės stebėsenos duomenų klasifikavimo modelių sukūrimui ir apmokymui buvo panaudotas atraminių vektorių klasifikatorius su radialine bazės funkcijos branduoliu ir dirbtinis neuroninis tinklas. Rezultatai parodė, kad sukurtas MM algoritmas leido 4,5 % pagerinti informatyvių ir neinformatyvių epizodų identifikavimo tikslumą (nuo 77,58% iki 84.35%). Tačiau svarbiausia išvada yra ta, kad esant informatyviems fiziologiniam AKS ir IKS pokyčiams, galima automatiškai identifikuoti optSPS(t) vertes per 10 kartų trumpesnį laiką (per 20-30 min.) lyginant su šiandien klinikinėje praktikoje naudojamomis technologijomis. Tolimesni perspektyviniai klinikinių tyrimai yra būtini siekiant labiau ištirti sukurtų MM algoritmų taikymo galimybes klinikinėje praktikoje.

Acknowledgements

All studies are supported by the Research Council of Lithuania (Grant No. MIP-20-216), the Research and Innovation Fund of Kaunas University of Technology project (Grant No. PP54/203), and the Research Fund of Lithuanian University of Health Sciences (Acronym: OptSPS-DI).

I would like to acknowledge a number of people who have helped me throughout this project and made it possible. First, I would like to thank my supervisor, Vytautas Petkus, for his continuous guidance and teaching. Second, I would like to thank Edvinas Chaleckas for his patience, support, and good laughs throughout this process. Third, I would like to thank Mindaugas Kavaliaskas for his machine learning expertise and contributions, without which, this project would not have been possible. Fourth, I would like to thank Arminas Ragauskas and all the members of the Cerebrovascular Autoregulation Lab. Fifth, I would like to thank my mother for her continual encouragement and support. Finally, I would like to thank Jake Liscow, I could not have done this without you.

List of Contents

List of Figures

List of Tables

List of Abbreviations

Abbreviations:

ABP- Arterial blood pressure;

Acc- Accuracy;

ANN- Artificial neural network;

AUC- Area under the receiver operator curve;

CA- Cerebrovascular autoregulation;

CBF- Cerebral blood flow;

CPP- Cerebral perfusion pressure;

CPPopt- Optimal cerebral perfusion pressure;

GOS- Glasgow Outcome Scale;

ICP- Intracranial pressure;

LLCA- Lower limit of cerebrovascular autoregulation;

MAP- Mean arterial blood pressure;

ML- Machine learning;

PRx- Pressure reactivity index;

RBF- Radial basis function;

Se- Sensitivity;

Sp- Specificity;

STD- Standard deviation;

SVM- Support vector machine;

TBI- Traumatic brain injury;

TF- Transfer function;

ULCA- Upper limit of cerebrovascular autoregulation;

Introduction

Traumatic brain injury (TBI) is a major global health concern that generates a significant burden on society through mortality, disability, socioeconomic losses, and reduced quality of life [1, 2]. In an acute medical setting, survival after TBI primarily depends on maintaining stable cerebral perfusion pressure (CPP) by ensuring patients receive adequate cerebral blood flow (CBF) [3, 4]. The Brain Trauma Foundation guidelines recommend a target CPP range of 60-70 mmHg to prevent secondary injuries caused by cerebral ischemia or edema [2]. However, this universal target range for CPP may not be the optimal value for the diverse scope of patients affected by TBI. Many factors can influence individual optimal CPP range including age, intracranial pressure (ICP), brain injury severity, glucose levels, and the duration of cerebrovascular autoregulation impairment events [5].

One method for CPP-targeted treatment is based on both determination of the cerebral pressure reactivity index (PRx), as well as identification and maintenance of the patient's optimized CPP value [6, 7]. PRx defines the correlation between slow moving ICP and arterial blood pressure (ABP) waves over a defined moving time window [8, 9]. ICP is most often measured invasively through surgical implantation of a micro transducer into intraparenchymal tissue or a catheter into one of the brain's ventricles [9, 10]. ABP can either be measured invasively through a sensor inserted into the radial artery or non-invasively through photoplethysmography [9, 10]. In clinical practice, PRx is the most commonly used assessment method for cerebrovascular autoregulatory status [2, 6].

Plotting PRx against CPP generates a U-shaped curve, with the minimum of this curve known as 'CPPopt', representing the value at which cerebral autoregulation is functioning optimally [8, 9]. CPPopt is a dynamic and patient-specific value [6]. Numerous retrospective studies provide support that maintaining CPP close to individual CPPopt values results in improved TBI patient outcomes [3, 11, 12]. However, considerable limitations challenge the practical application of CPPopt-informed treatment strategies [6, 9]. Artifacts caused by patient movement, the disappearance and/or low amplitude of slow waves, the influence of general anesthetics [13, 14], patient status dynamics [13], and other physiological factors can distort the monitoring data [9]. This reduces usable data by 40–50% [8, 15], making it unreliable and sometimes impossible to identify CPPopt values for all patients when confounding factors are present [6, 9]. The identification of CPPopt can also be interrupted by different physiological processes accruing within an ICP and ABP monitoring window, as this requires a more complex analysis. In turn, accurate human recognition and interpretation of this intricate data requires extensive education and training of TBI physiology, which can be difficult to acquire. Due to these challenges, typical CPPopt calculations require at least 4 hours of continuous patient monitoring data [2]. This extended length of time prior to medical treatment can be critical as evidence suggests cerebrovascular impairment lasting longer than 30 minutes significantly reduces positive outcomes [6, 16, 17].

Machine learning (ML) approaches such as support vector machines, artificial neural networks, and decision trees have already shown promising results in clinical decision making [18–21]. Most existing models in TBI research have used inputs from various brain imaging techniques and physiological parameters to look for associations between variables and long-term outcomes with success [22–24]. There are a growing number of studies showing strong evidence that ML algorithms outperform common predictive models of TBI patient outcomes [21, 25, 26]. Yet, the impact of ML algorithms used to identify individualized CPPopt targets has not been explored.

The **aim** of this research is to develop and validate an ML algorithm to identify individual CPPopt values for TBI patients using only informative data.

The **objectives** are:

1. To develop a database of retrospectively analyzed patient physiological monitoring episodes that clearly distinguishes ‘informative’ data from ‘non-informative’ based on the presentation of critical events in ABP and ICP slow-wave forms.

2. To develop a machine learning algorithm which learns to identify individual patient CPPopt values from selected ‘informative’ episodes classified based on data presented in ABP and ICP slow-wave forms.

3. To test the possibility of identifying individual patient CPPopt values in monitoring time windows under 30 minutes.

1. Background

1.1. Physiology of Traumatic Brain Injury

This chapter presents background information about traumatic brain injury, current monitoring methods, and the relevance of treatment challenges in a clinical setting.

1.1.1. Cerebrovascular Autoregulation

Cerebrovascular autoregulation (CA) is the brain's ability to regulate and maintain cerebral blood flow (CBF) despite changes in cerebral perfusion pressure (CPP) [9, 27], defined as:

$$CPP = Mean\ Arterial\ Blood\ Pressure\ (MAP) - Intracranial\ Pressure\ (ICP) \quad (1)$$

Upon assessment, CA can be further characterized into static and dynamic autoregulation [27, 28]. Static CA quantifies only steady state relationships between CBF and MAP without considering the time it takes for these changes to occur [28, 29]. Dynamic CA represents the rate at which these dynamic changes take place between CBF and MAP [9, 27, 28]. The assessment of dynamic CA is based on the premise that after a change in MAP, CBF will react to the change before returning to its original value [28, 29]. The faster CBF returns to normal, the healthier CA is functioning. The concept of CA was first proposed by Lassen [30] in 1959 as a triphasic curve, illustrated in **Fig. 1**. The curve consists of the lower limit, plateau, and upper limit of autoregulation [9, 27]. Since its development, this triphasic curve has been adopted into modern CA modelling. In a healthy adult, functioning CA limits are between 50 and 150 mmHg CPP or 60 to 160 mmHg [9]

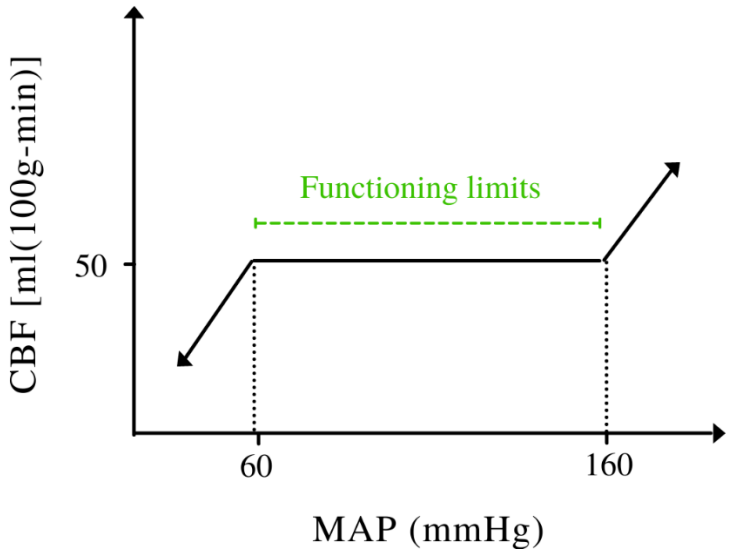

Fig. 1. Lassen's triphasic curve of cerebrovascular autoregulation

Steady ICP requires a balance of fluid components in the intracranial cavity, consisting of blood and cerebral spinal fluid (CSF) [10]. This requires coordination between the inflow of arterial blood and the outflow of venous blood, balanced with the rate of CSF production and drainage. The fluid exchange in the intracranial cavity is illustrated in **Fig. 2.** CA ensures that as MAP or CPP increases, vasoconstriction of the cerebral arteries reduces blood flow to the brain to prevent cerebral edema by hypo-perfusion [9, 27, 31]. Conversely, this process maintains steady ICP through vasodilation of the cerebral arteries when MAP or CPP decreases to increase blood flow and prevent ischemia [31].

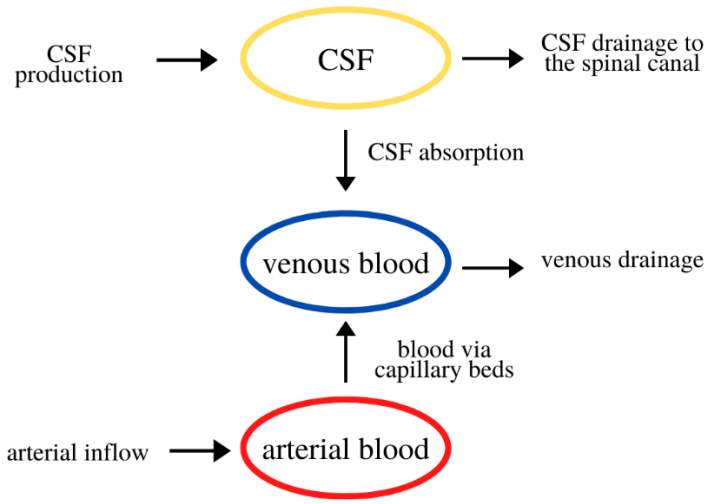

Fig. 2. Fluid balance in the intracranial cavity affecting intracranial pressure

1.1.2. Traumatic Brain Injury and Cerebrovascular Autoregulation Dysfunction

A traumatic brain injury (TBI) is defined by the Brain Trauma Foundation as "a sudden trauma, often a blow or jolt to the head, which causes damage to the brain" [32]. Receiving a TBI can impair CA function, meaning the brain is unable to maintain CBF within the upper and lower limits of autoregulation. With a lack of mechanisms to prevent it from dipping, CPP can easily decrease below the lower limit, rapidly leading to cerebral ischemia [27, 31]. In a state of ischemia, the brain lacks adequate oxygen and nutrients, drastically increasing the possibility of secondary injuries in the cerebral tissue and compromising the likelihood of functional recovery [9, 27].

Conversely, when CA is impaired and there is no regulatory mechanism preventing it from rising, CPP can swiftly increase above the upper limit, resulting in swelling of the brain known as cerebral edema [27, 31]. The combination of CSF and blood begins to pool inside the cranial cavity; with the brain encased in the skull, it has no room to expand and ICP can increase to dangerously high pressures. Left untreated, cerebral edema can cause disruption of the blood brain barrier, neurological complications, and eventually death [9, 27, 33].

The potential consequences of CA impairment following TBI are illustrated in **Fig. 3.** The green line represents healthy functioning CA, which remains relatively constant within the lower and upper bounds of CA, as CPP and MAP fluctuate [33]. The red line illustrates impaired CA function, which can lead to ischemia and edema, along with their corresponding secondary injuries [33].

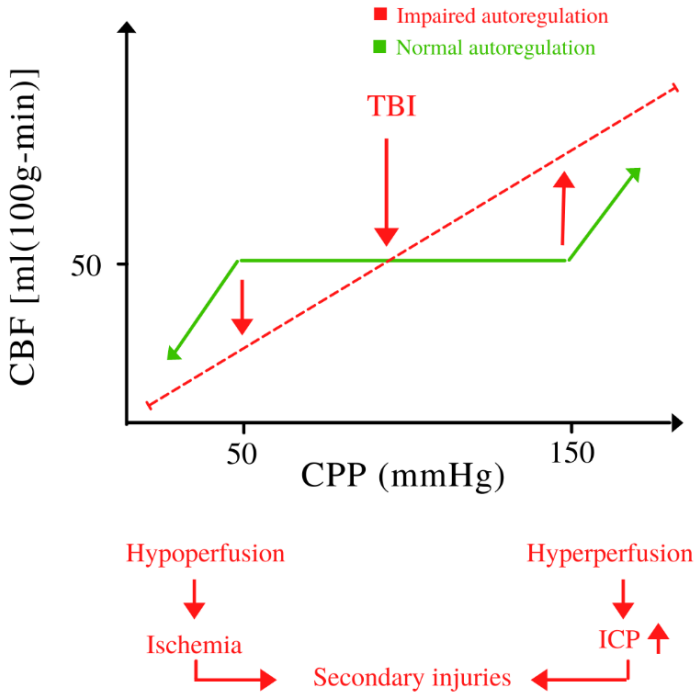

Fig. 3. Autoregulatory curve with CA dysfunction caused by TBI [33]

1.2. Technology of TBI Patient Monitoring and Treatment

This section describes current technologies used in clinical practice to monitor and assess cerebrovascular autoregulation in TBI patients.

1.2.1. Cerebrovascular Autoregulation Monitoring

Over the last 20 years, a wide variety of techniques have been developed and applied for CA monitoring and assessment [34]. To name a few: Transcranial Doppler (TCD) ultrasound, functional Near Infrared Spectroscopy (fNIRS), brain tissue oxygenation, parenchymal ICP monitors, and extra ventricular catheters [34]. Along with each of these monitoring methods, indices to assess CA have been created, such as the mean flow index (Mx), volumetric reactivity index (VRx) [35], and pressure reactivity index (PRx) [5, 34]. Today, using PRx for CA assessment is the clinical standard [2, 5, 34].

PRx describes the ability of cerebral vessels to change their diameter in response to fluctuations in ABP, while maintaining a stable CBF [12]. This index is calculated as the Pearson correlation coefficient between ABP and ICP slow waves [5]. Slow waves are oscillations in ABP and ICP that are longer than those stimulated by physiological respiratory responses [36]. Waves can be classified as slow waves when all components have a spectral representation within the frequency limits of 0.05–0.0055 Hz [36, 37]. Rhythmical changes in CBF are directly translated into ICP slow waveform, where increased slow wave amplitude indicates an exhausted CA response [37].

ICP is continuously measured most accurately through invasive surgical implantation of either a micro transducer into intraparenchymal tissue, or a catheter into one of the brain ventricles [34]. ABP is measured by a sensor inserted into the radial artery or non-invasive photoplethysmography [9, 34]. To establish PRx estimates, mean ICP and MAP values are calculated every 10 seconds to 3 minutes [38], followed by a correlation of 30–40 consecutive values [9]. PRx values range from -1 to 1. A negative value of PRx reflects normal cerebrovascular reactivity, while a positive value indicates

dysfunction [3, 9, 38]. **Fig. 4** illustrates the relationship between ABP and ICP slow wave forms and their reflected values in PRx. It is important to bear in mind that the reliable estimation of PRx values requires the presence of spontaneous fluctuations in ABP wave forms [16]. While such fluctuations are present in most patients following TBI, the magnitude of these fluctuations may be insufficient to produce significant ICP changes. In these cases, it is either not possible to calculate PRx or the determined value will be unreliable [38].

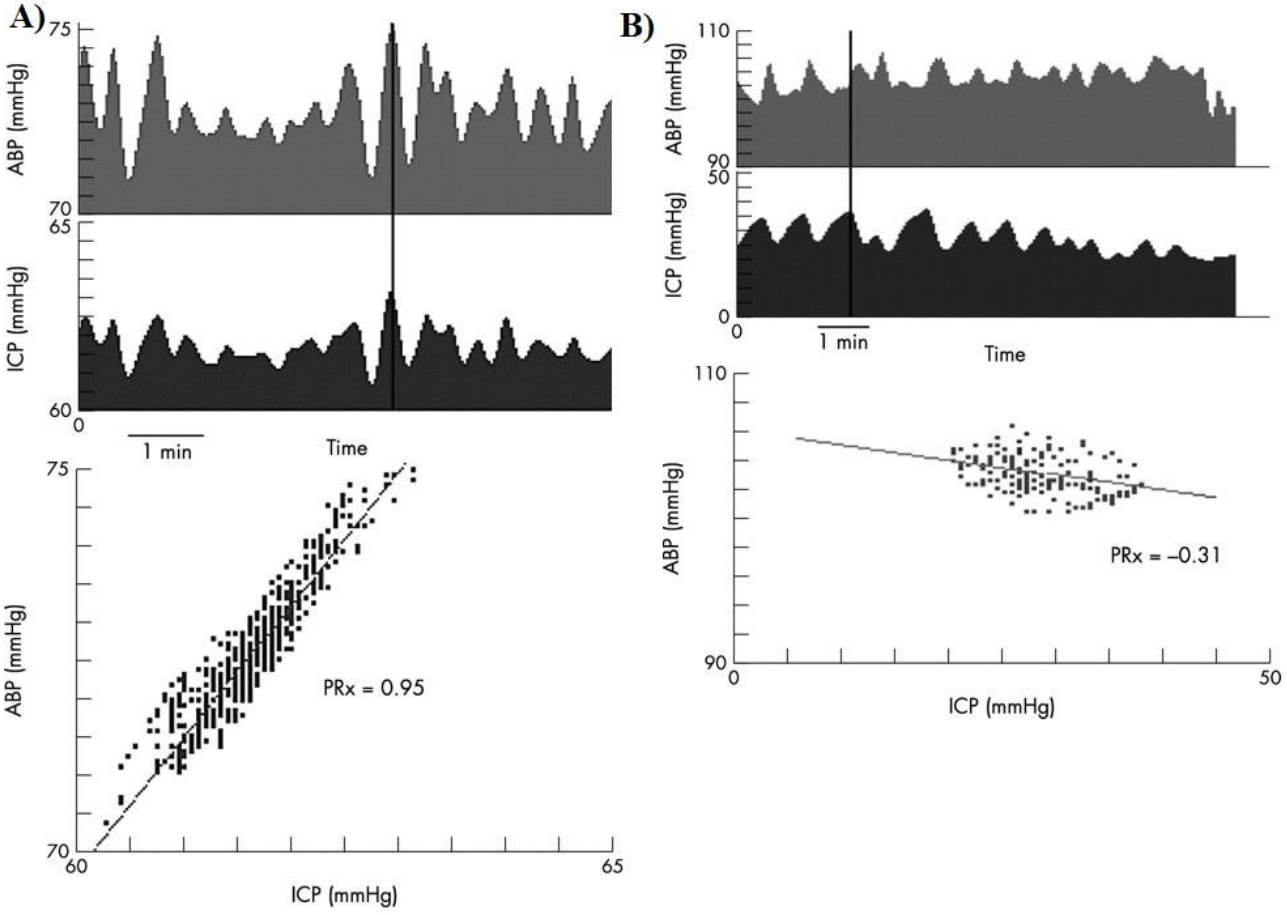

Fig. 4. The relationship between ABP and ICP slow waves and PRx value [57]

The black line in both A) and B) illustrate the slice of ABP and ICP data reflected on associated PRx graphs. A) illustrates a positive correlation between slow waves in ICP and ABP, resulting in a positive PRx value. This indicates loss of cerebrovascular reserve and impaired CA [38, 57]. B) illustrates a negative correlation between slow waves in ABP and ICP, resulting in a negative PRx value. This indicates healthy cerebrovascular reserve and functioning CA [57].

PRx values represent the average of all intracranial vascular regions and can be described as a global CA-related index [38, 39]. As the brain is complex and all regions do not work in unison, it requires varying CPP values depending on individual demands [39]. For example, an area of the brain that is uninjured will likely require a normal CPP, while areas that surround a hemorrhage will require varying CPP values. In addition, it is assumed that slow wave ICP oscillations are vasogenic in nature, when this is not always true. In this way, the PRx is an oversimplification of the myogenic mechanisms that work to maintain adequate cerebral blood flow and does not include the metabolic and neurogenic contributions [39, 40].

1.2.2. Optimal Cerebral Perfusion Pressure

The abundance of cerebrovascular autoregulation monitoring and assessment techniques available can increase complexity for clinical decision making, with considerable variation in research methodology [5, 34]. There is evidence that maintaining a TBI patient's CPP within the range of 60–70 mmHg leads to improved patient outcomes [2, 6, 7, 9, 11]. However, knowing which CPP is ideal for a specific patient can be difficult — too low and too high risk falling outside the patient's individual lower and upper limits of CA [39].

One proposed method is to find an individualized 'optimal' CPP, known as 'CPPopt', which combines continuous monitoring of CPP and PRx values [6, 9]. This value is identified as the minimum CPP value of the U-shaped relationship between PRx and CPP, illustrated in **Fig. 5**. CPPopt-targeted treatment is based on the premise that CA stability can be preserved if CPP is kept away from the dynamic lower and upper limits of autoregulation [2, 9]; this value represents an individual target for clinicians to achieve optimally functioning CA [9]. CPPopt is dynamic, differs between patients, and ranges within an individual's triphasic CA curve over time [3, 6]. There is a growing number of retrospective observational studies showing evidence of the effectiveness of CPPopt-targeted treatments through association between poor outcome and deviation from calculated CPPopt [6, 9, 41, 42] but there lacks prospective clinical evidence [2, 11].

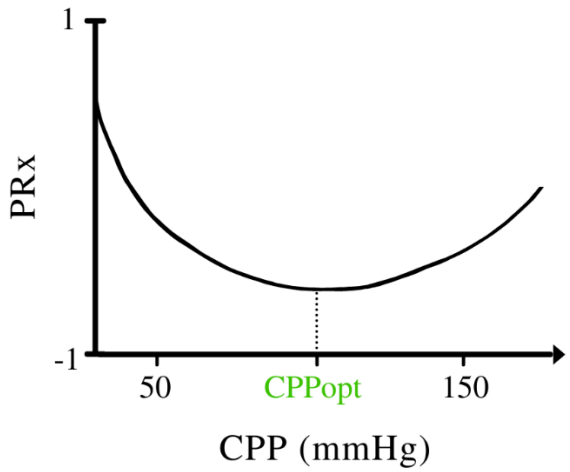

Fig. 5. Graph of CPP vs PRx used to identify CPPopt

Two prospective pilot studies have been performed to date, both providing support for the effectiveness of CPPopt-targeted treatment. The first, completed in 2010 by Jaeger et al. [12], attempted to evaluate PRx-guided CPPopt values following TBI by analyzing the relationship between CPPopt and brain tissue oxygen for 38 brain injury patients. The results of the study presented a significant correlation between CPPopt and CPP values, where brain tissue oxygen reached its plateau ($r = .79$, $p < .01$). Accordingly, the study supported the use of PRx in CPPopt-targeted treatment for TBI patients, warning of the risk of secondary injuries above or below this calculated value. The second study, performed in 2015 by Dias and associates [11], assessed the outcome of CPPopt-based treatment using PRx over a 4-hour time window. The study demonstrated that patients with a difference of more than 10 mmHg between real CPP and CPPopt were more likely

to have poor outcomes ($p = 0.04$). Thus, the authors concluded that CPPopt-targeted treatment for TBI patients seemed feasible.

In addition, the feasibility and safety of CPPopt-targeted treatment is currently being evaluated in the first prospective, multi-centre, randomized, controlled trial underway by Beqiri et al. [43], titled "CPPopt Guided Therapy: Assessment of Target Effectiveness (COGiTATE)".

1.2.3. Challenges in Patient Monitoring and Treatment

There are numerous challenges for current CPPopt-targeted methods, culminating in a 40–50% reduction in usable and informative data [6, 9]. Factors that can render monitoring windows non-informative include a range of artifacts that can degrade the signal-to-noise ratio of the data collected. Artifacts can be the result of a multitude of reasons including the influence of general anesthetics [14, 44, 45], patient status dynamics [44], changes in monitoring equipment setup [9], along with the malfunctioning of these technologies [9]. Even routine patient manoeuvring by the nurse [9] and simple patient movements such as coughing, sneezing, and using the bathroom can reduce the usability of collected data signals [3]. Another important factor to consider is the patient risk associated with the invasive nature of ICP monitoring. Additionally, the disappearance of ICP slow waves or insufficient amplitude of ICP slow waves [35] makes it impossible to calculate PRx or CPP values. Some of these challenges can be mitigated by halting PRx calculations during manoeuvres and equipment changes, but there is no way to prevent all artifacts from happening. Due to the overwhelming number of factors that negatively affect the data quality, the typical monitoring time window must be at least 4 hours in length to gather enough data to estimate CPPopt and PRx values [9]. Few studies have investigated the use of a shortened time window [8, 46] in these calculations, as this subsequently reduces the percentage of usable data [4, 11].

In 2014, Depeitrere et al. [8] led a retrospective study to investigate how the processing of patient data to calculate PRx values could be obtained from minute-by-minute ICP and MAP low frequency data, rather than the standard high frequency data. To accomplish this, the team created a low frequency index called LAx and calculated the associated CPPopt values. These values were compared in a multivariate logistic regression ($n = 180$) against the corresponding CPPopt values, calculated using PRx. The results showed that when using the LAx, CPPopt values could be identified in 95% of the monitoring time and that achieving a patient's actual CPP close to LAx-based CPPopt was associated with increased long-term survival rates. The study concluded that it was possible to assess CA status and identify CPPopt values based on minute-by-minute ICP/MAP data, which contained relevant information for calculations.

1.3. Machine Learning

Supervised machine learning (ML) models such as artificial neural network (ANN), support vector machine (SVM), and decision trees are already being implemented in TBI research with the goal of improving patient outcomes.

1.3.1. Artificial Neural Networks

ANNs are universally applied supervised ML methods that excel in classification and pattern identification [18, 24, 47]. When used for classification models, an ANN can be thought of as a set

of interconnected inputs and outputs, each connection uniquely weighted to represent the strength of the connection [47, 48]. Data for ANN optimization is separated into training and testing data sets, with the training data being used iteratively until errors are minimized [21, 49]. A trained ANN can be used effectively to predict future outcomes [20, 21, 24, 47].

1.3.2. Support Vector Machines

SVM is a type of supervised ML that works to classify both linear and non-linear data sets [21, 47]. These models are based on the idea of finding a hyperplane which best separates and classifies two data sets. The key when using SVM for classification models is to determine which kernel function (linear, nonlinear, polynomial, radial basis function, or sigmoid) will best achieve the most distinct hyperplane or decision boundary to separate the two discriminative groups [21, 47]. SVM can be trained and the hyperparameters optimized to successfully predict TBI patient outcomes based on feature identification [48].

1.3.3. Applications in TBI Research

Studies applying ML to TBI research to date have primarily focused on implementing ML models for feature identification from radiological images and using this information to predict long-term patient outcomes [22, 24, 25, 50]. Many studies investigating the use of ML models in TBI research have concluded that SVM is the best classifier and produces a higher prediction accuracy than other models [21]. Other studies suggest that ANN is the best predictor of TBI patient mortality [24]. It is important to note that all to my knowledge, no previous studies have investigated the use of ML to identify individual CPPopt and limited studies have used a shortened continuous monitoring time window under 4-hours for these calculations. The lack of research in the use of ML in bedside TBI patient management emphasizes the need for further investigation and the construction of data repositories, including continuous patient physiological signals. Modeling strategies must constantly be improved to include external validation. Prediction models based on the wide range of supervised ML models need continuous validation to ensure their effectiveness [24, 25, 50, 51]

To summarize, TBI is a global health concern that needs to be addressed immediately to reduce stress on societal systems and resources. Treatment methodologies based on optimizing CPP values are proven to be effective, yet this still contain limitations which prevent patients from receiving personalized medical intervention within their critical time frame. This research aims to apply modernized machine learning tools to address this problem by more reliably identifying individualized treatment targets for TBI patients.

2. Methodology

This chapter presents the methodology of the work, including patient data, a description of the physiological data signals collected, the implementation of the proposed algorithm, and methods for performance evaluation. The methodology is presented in **Fig. 6** as a flow diagram**.**

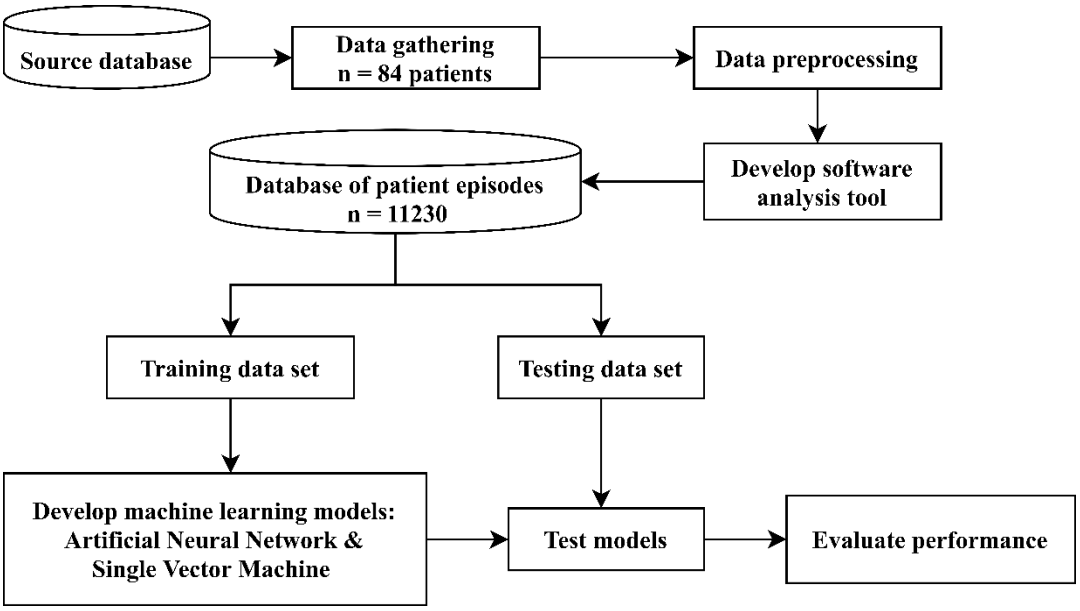

Fig. 6. Project methodology overview

2.1. Patient Data and Physiological Parameters

All studies were approved by the Vilnius and Kaunas Regional Biomedical Research Ethics Committees (protocols No. 158200-06-498-145, 158200-16-854-364, 2016- 07-12, 158200-15-801-323, 2015- 10-06 and BE-2-6, 2015-01-06).

This research contained a retrospective analysis of multimodal physiological monitoring data of 84 severe TBI patients. The data were collected in the Republican Vilnius University Hospital ICU and Lithuanian University of Health Science Kaunas Clinic from clinical studies throughout 2013 to 2018. High-resolution continuous monitoring data of ICP(t), ABP(t), CPP(t), and PRx(t) were registered and calculated using ICM+ Cambridge Software. ICP data signals were collected using Codman monitors with ventricular or parenchymal sensors. ABP signals were collected using Datex Ohmeda monitor with pressure sensor in the radial artery.

Patient outcome was evaluated six months following hospital discharge by the Glascow Outcome Scale (GOS) [19], defined as:

Table 1. Glasgow Outcome Scale

Score	Functional Status	Description
5	Good recovery	Resumption of normal life despite minor deficits
4	Moderate disability	Disabled but independent; can work in a supported environment
3	Severe disability	Conscious but disabled; dependant on others for daily support
2	Persistent vegetative state	Minimal responsiveness
1	Death	Self-explanatory

2.1.1. Signal Preprocessing

ICM+ software collects patient data signals and performs real-time calculations. PRx was calculated as the moving correlation coefficient between the patient's ABP and ICP slow waves. This is the averaged value over the monitoring window when CPPopt has a minimum PRx value. A 10-second moving average filter was implemented on all acquired signals to filter out pulse and respiratory waves, which can cause interference. The initial sampling frequency of raw APB and ICP data was 300 Hz, as defined by ICM+ software standards [51]. To reduce the computational complexity of the system and decrease the time required for signal processing, these signals were decimated to a sampling frequency of 0.1 Hz.

For dynamic CA analysis, transfer function analysis (TFA) was performed. Fast Fourier Transform was first applied to compute the spectral analysis in the frequency domain. Then, both auto- and cross-spectrum analysis were applied to obtain estimates of coherence and gain frequency responses in the specific low range of 0.005–0.02 Hz.

2.2. Database Construction

The first objective of this research was to create a database of patient monitoring episodes that could be later used to train the proposed ML model. To do so, a unique software tool was developed using MathWorks MATLAB [53] running on Microsoft Windows 10. The primary purpose of this tool was to illustrate, analyze and annotate patient physiological data from ICM+ Software [52] over 2-hour monitoring windows. The monitoring data from 84 patients created 2,165 2-hour time windows. Each window was further divided into 5 episodes of roughly 24 minutes in length, which created 11,230 episodes for the training database. The selection of 24 minutes time for episode deconstruction was determined due to the agreement that CA impairment lasting longer than 30 minutes can be critical to a TBI patient [6, 16, 17]. The data base created from the CPPopt software tool contained 8,398 episodes which were annotated as 'informative' and 2,427 as 'non-informative'. Of these episodes, 70% were used in the development of the MATLAB CPPopt Software Tool and the training of the proposed ML algorithm. The remaining 30% of episodes were reserved for testing data after the proposed ML model was created.

2.2.1. CPPopt Analysis Software Tool

The developed CPPopt analysis software tool required one input: physiological patient monitoring data from ICM+ software. This tool illustrated the input data over 6 graphs on the user monitoring screen. The 3 graphs on the left side of the user screen are the variables ABP, ICP and PRx as a function of time over the 2-hour monitoring window shown on **Fig. 7**. The 3 graphs on the right side of the user screen as the PRx values calculated from the variables CPP, ICP and ABP shown on **Fig. 8**. These functions are defined by equations (2), (3) and (4).

$$PRx = f(CPP) \tag{2}$$

$$PRx = f(ICP) \tag{3}$$

$$PRx = f(ABP) \tag{4}$$

To identify CPPopt values, second-degree polynomial approximations were applied and the minimum point on the U-shape curve was recorded. The addition of equations (3) and (4) were included under

the assumption that they would enable a deeper analysis of how ABP and ICP were limiting in the identification of CPPopt. Optimal values of ABP and ICP were calculated under the same assumption. CPPopt, ABPopt and ICPopt represented the targeted CPP, ABP and ICP treatment values for each individual patient episode. Additionally, the lower and upper limits of CA (LLCA and ULCA, respectively) were calculated for CPP, ABP and ICP at the PRx threshold of +0.25.

2.2.2. Classification

To distinguish each 24-minuite episode from the 2-hour monitoring window, colours were assigned to each episode along the timeline in green, cyan, blue, pink, and red. Comprehensively trained medical physicists from the Vilnius and Kaunas clinics performed a thorough analysis of all patient data monitoring episodes. The annotation of 'informative' and 'non-informative' data segments was indicated by either selecting or deselecting each episode colour. Episodes were classified as 'informative' if they contained slow-wave oscillations in ICP and ABP signals within the frequency range of 0.05-0.0055 Hz or when an identifiable U-shaped curve was presented in the CPP vs PRx graph. Episodes were classified as 'non-informative' if they contained missing data, a sudden drop in the difference between systolic and diastolic ABP data, or rapid changes in ICP/ABP data. If there was any unclarity is classification, the episode was annotated as 'non-informative'. Additionally, one of five clinical situations was selected as defined as:

Table 2. Five clinical situations and recommended treatment

Number	Label	Reason	Recommended treatment
1	CPP TH	U-shape or lower and upper limits of CA are identified in CPP data	CPP- based therapy is recommended
2	ABP TH	U-shape or lower and upper limits of CA are identified in ABP data	ABP-based therapy is recommended
3	ICP TH	U-shape or lower and upper limits of CA are identified in CPP data	ICP-based therapy is recommended
4	CA Crit	PRx is above 0.25 for all values of CPP	CA is critical and requires immediate treatment intervention
5	CA OK	PRx is below 0.25 for all values of CPP	CA is stable and no specific treatment or management is necessary

The CPPopt software tool produced one main output: a data set of patient monitoring episodes, each annotated as either 'informative' or 'non-informative' and marked as one of the predefined clinical situations. The input and outputs of this tool are summarized in **Table 3**.

In **Fig. 7**, the pink data section is marked as informative because the waveform presented during this episode is enough to identify a U shape in the CPP vs PRx graph. The remaining data section colours remain unmarked as they are 'non-informative'. The result is that CPPopt and both the lower and upper limits of CA have been identified. Therefore, CPPopt-targeted treatment is necessary for this patient episode and is annotated on **Fig. 8**. Each colour is associated with the associated sections marked. Buttons were included to select or deselect each colour for inclusion in the graphs and calculations. In this example, all colours are selected on the graph represent data from the full 2-hour monitoring window.

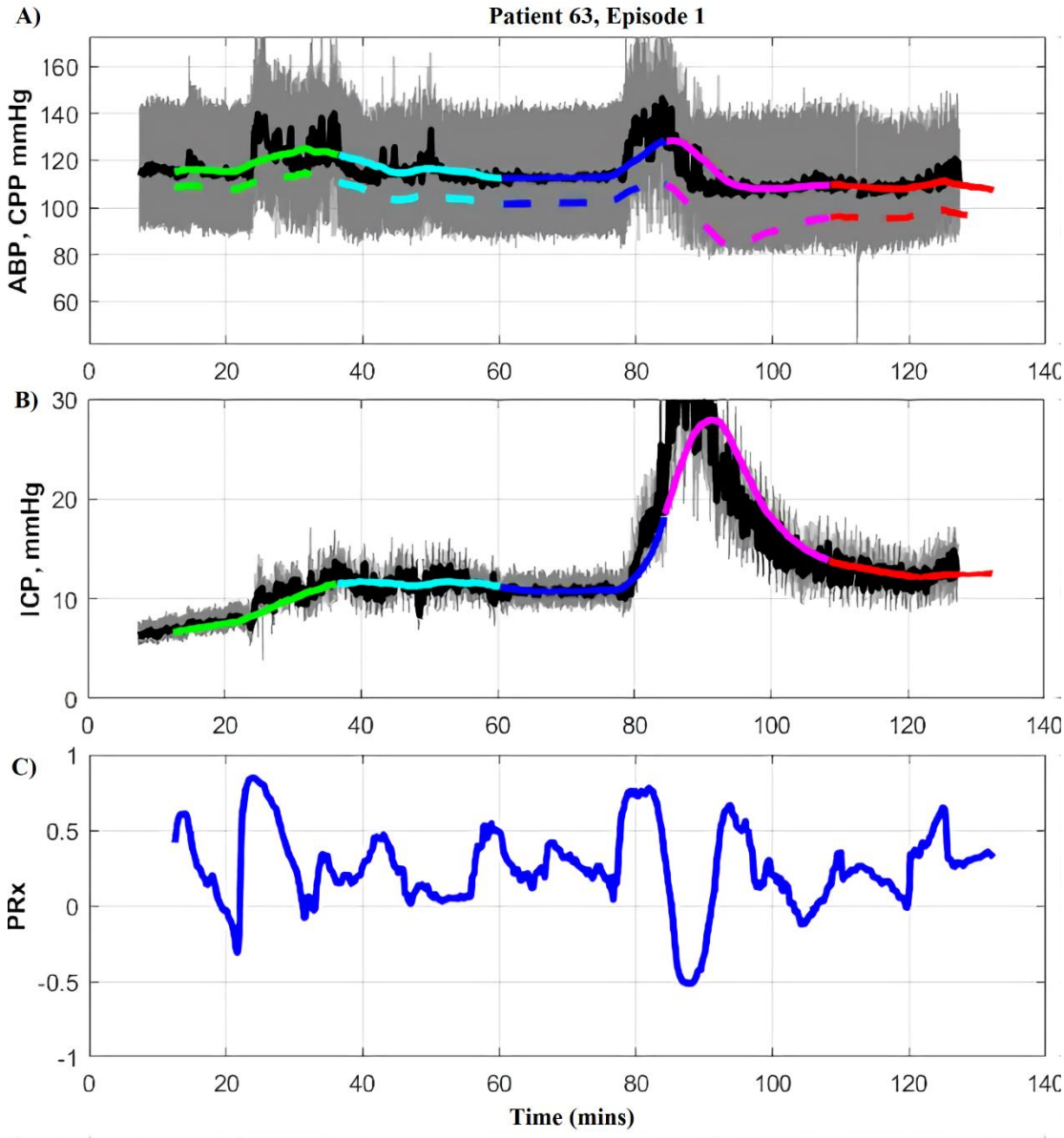

Fig. 7. CPPopt Software Tool: Patient 63, Episode 1 (left side of screen)

Graphs A, B, and C illustrate variables ABP, ICP, and PRx as a function of time (min) over 2 hours. Graph A) illustrates ABP (mmHg) and CPP (mmHg). In this episode, the informative section is highlighted in pink around the 90-minute mark. B) illustrates ICP (mmHg) over the monitoring window. Here, the cerebrovascular autoregulatory response is seen in the highlighted pink section around 90 minutes and C) illustrates the PRx values calculated with association ABP and ICP values. Around 90 minutes, the PRx value decreases to -0.5. This value is indicative of a healthy autoregulatory response and further supports the highlighted pink episode.

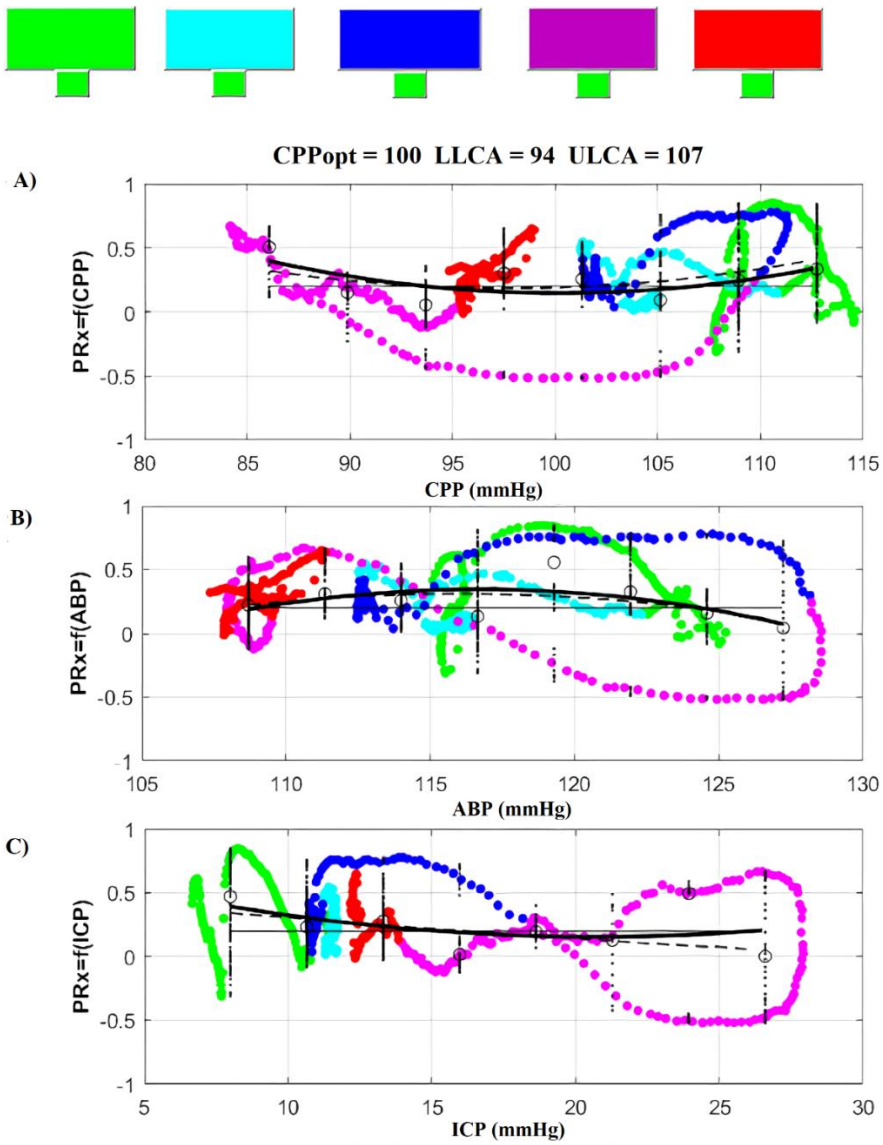

Fig. 8. CPPopt Software Tool: Patient 63, Episode 1 (right side of screen)

A) illustrates the PRx values calculated from CPP values over the monitoring window. Highlighting solely the pink episode, it is easy to visually identify a U-shaped curve, indicating that it is possible to identify the individual CPPopt value for this patient's particular episode using only the pink data episode. Graph B) illustrates the PRx calculations based on ABP values and C) illustrates the PRx values calculated based on ICP. From this analysis, pink was annotated as an 'informative' episode, and the remaining 4 episodes were marked 'non-informative'.

Table 3. CPPopt software tool input and outputs

Input	
1	Raw ABP, ICP, CPP and PRx data signals from ICM+ software
Output	
1	Each 24-minute episode annotated as 'informative' or 'non-informative' (1,0)
2	Each 24-minute episode annotated as specific clinical scenario defined in **Table 3**

2.3. Proposed Machine Learning Algorithm

Two supervised ML models were utilized to develop the proposed algorithm using R: A Language and Environment for Statistical Computing [53, 54]. Dr. Mindaugas Kavaliaskas, a fellow from the

mathematics department of Kaunas University of Technology, significantly contributed to the designing and building process of the proposed ML algorithm. ANN and SVM models were selected to provide a baseline comparative performance; both models were trained using the same training data. All data stored in the database was separated into 70% training data (n = 8984) and 30% testing data (n = 2246).

Throughout the preliminary stages of the ML algorithm development, when comparing cross validation accuracy been the two models, the SVM method yielded better results (Acc = 66.8%) compared to the ANN method (Acc = 60.8%) in the prediction of informative and non-informative episodes. Therefore, the methodology will focus on the development of the SVM method. The steps taken to design the proposed ML algorithm are illustrated in **Fig. 9** and are further explained throughout this chapter.

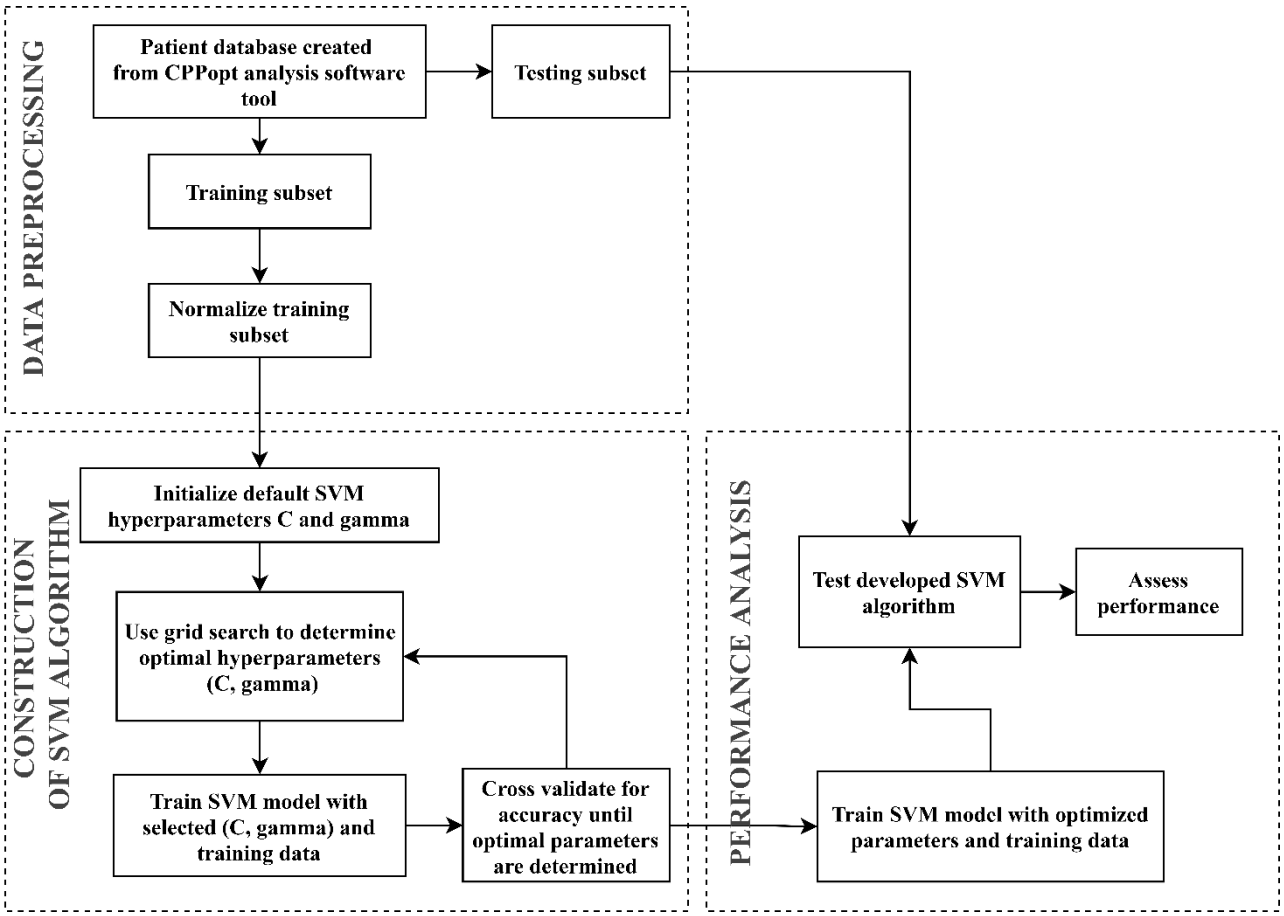

Fig. 9. Flow chart of the developed ML algorithm

2.3.1. Design

The proposed ML algorithm was created using R Programming Language's SVM function as a part of the e1071 package. The training dataset used to build the SVM model was extracted from the previously created patient episode database. The goal of the SVM model was to optimize the hyperplane, also known as decision boundary, between 'informative' and 'non-informative' classifications. To accomplish this, a radial basis function kernel was used to transform the training data to a hyperplane on a high dimensional feature space. Data points falling on either side of the hyperplane were attributed to the two different categories. Episodes that were more challenging to distinguish between 'informative' and 'non-informative' were penalized as their classification

would directly affect the optimal decision boundary. The SVM optimization problem can also be called the convex quadratic optimization problem.

2.3.2. Parameter Optimization

The next step was to optimize the hyperparameters using the training data: Cost (C)- the slack variable cost; and gamma (γ)- the width of the radial basis function. The hyperparameter C indicates to the SVM how much to avoid misclassification by adding a penalty for each misclassified data point. When C is small, the penalty is low, so the SVM will choose a large decision boundary margin with the expense of more misclassifications. On the other hand, if C is large, the penalty is large so the SVM tries to reduce the number of misclassified points. This results in a smaller margin on the decision boundary. The penalty is different for each data point and is directly proportionate to the distance to the decision boundary.

The hyperparameter γ determines how much complexity or curvature is included in the decision boundary by controlling the distance of influence of a single training point. Larger values result in the decision boundary radius being too large and include all data points as highly penalized support vectors. Conversely, if γ is too small, the decision boundary in constrained and unable to capture the complexity of the data spread, meaning that the data points need to be particularly close together to be classified in the same group.

C and γ were initialized by their default values recommended in R documentation for the SVM defined by:

$$C = 1 \tag{5}$$

$$\gamma = \frac{1}{\| x \|^2} \tag{6}$$

The optimal combination of C and γ were selected through iterative grid search with exponentially growing factors (0.001, 0.01, 0.1, 1, 10, 100, and 1000). The grid search trained the SVM model with each hyperparameter pair (C, γ) as the Cartesian product of these two sets, and evaluated their performance using cross-validation to determine the highest accuracy. A set of different ordered values were compared with the optimal set of parameters because the scale of these parameters is difficult to guess in advance. During testing, default parameters were close to optimal, indicating that a different grid for selecting optimal C and γ values was required. The selected optimal parameters defined in equations (7) and (8) were up to 16 times larger and smaller than the default values and were used to train the entire training set and generate the final ML algorithm.

$$C = 2^{(-4:4)} \tag{7}$$

$$\gamma = 2^{(-4:4)} \tag{8}$$

2.3.3. Inputs and Outputs

After final design, the proposed ML algorithm required 3 inputs. First and primarily was patient physiological monitoring data from ICM+ software. This included ABP, ICP, PRx and CPP values

over the defined time window. Two additional inputs were created with the goal of improving classification accuracy of the proposed ML algorithm.

The second input was the inclusion of STD values for ICP and ABP data using 5 different moving average filters. This is based on the concept that data segments containing rapidly changing data are typically 'non-informative', as fast changes often signify an artifact. The STD is measure of how much the data varies from the mean and therefore, a data segment with a large STD is likely to have an artifact in it and can be assumed to be 'non-informative'. After applying a moving average filter to these high amplitude episodes, the STD decreases as the time window of the filter increases. In result, STD values remained unchanged or decreased slowly for informative data episodes which contain low amplitude slow waves when applying a larger moving average filter. Normalizing these values then produced a comparable metric ranging between 0 and 1. A normalized STD is defined by:

$$Normalized\ STD = \frac{STD(filtered\ data)}{STD(raw\ data)} \tag{8}$$

'Informative' data episodes are indicated by values close to 1 while 'non-informative' data episodes are close to 0. Identifying the largest normalized STD value was a key input factor that assisted the ML algorithm in discriminating between the two groups (0 = 'non-informative', 1 = 'informative'). Different time windows were used for moving average filters of 0 (no filter), 1, 2, 3, and 4 minutes to investigate which time window produced the largest differentiation between groups.

The third input was gain and coherence gathered from the TFA data. The gain represents the damping effect of CA on the magnitude of ABP oscillations [55], marking the efficiency of the autoregulatory response. A low gain signifies a healthy and stable CA, while an increase in gain signifies a diminished CA efficiency meaning the autoregulatory response in unstable and/or impaired. Coherence represents the linearity between the waveform before and after TFA. Coherence values close to 0 represent no relation, while values within a specific range suggest linear relation. However, low coherence values can also be indicative of extensive noise and artifacts in the signal. Therefore, patient episodes which contained a low coherence value were classified as 'non-informative'. For these reasons, TFA gain and coherence were included as inputs of the ML algorithm within a specific slow wave frequency range of 0.005–0.02 Hz.

There were three defined outputs from the CPPopt software tool which created the patient database. The first output contained patient episodes classified as 'informative' or 'non-informative'. The second consisted of patient episodes classified as one of five specific clinical situations. The third output included patients CPPopt, LLCA, and ULCA values calculated with 'informative' data episodes. Inputs and outputs are summarized in **Table 4**.

Table 4. Proposed ML algorithm inputs and outputs

Input	
1	Patient physiological monitoring data from ICM+ Software
2	Calculated standard deviation ratios of ICP and ABP signals for each patient window
3	Calculated transfer function analysis gain and coherence of ICP and ABP signals for each patient window
Output	
1	Patient 24-minute episodes classified as 'informative' or 'non-informative'

2	Patient 24-minute episodes classified as specific clinical scenario
3	CPPopt, lower limit of CA and upper limit of CA for each episode based on only 'informative' data

2.4. Evaluation Methods

The calculations and evaluation of performance parameters were completed using R: A Language and Environment for Statistical Computing (e1071 package). The performance parameters used in the evaluation were prediction accuracy (Acc), sensitivity (Se), and specificity (Sp), calculated with 2x2 confusion matrices. The true positive (TP) rate is the number of correctly predicted 'informative' episodes, while the true negative (TN) rate is the number of correctly predicted 'non-informative' episodes. The false positive (FP) rate is the number of incorrectly predicted 'informative' episodes, while the false negative (FN) rate is the number of incorrectly predicted 'non-informative' episodes. Sensitivity and specificity are defined in equations (9) and (10), respectively.

$$Se = \frac{TP}{TP + FN} \tag{9}$$

$$Sp = \frac{FP}{TN + FP} \tag{10}$$

Accuracy was calculated as the proportion of correct predictions for informative and non-informative over the total number of patient episodes, given by:

$$Acc = \frac{TP + FP}{TP + TN + FP + FN} \tag{11}$$

The model was accessed further with linear regression analysis and calculated Pearson correlation coefficients (r) using IBM SPSS Statistics. The dependent continuous variables in our study were CPP, ABP, and ICP, all of which were not normally distributed. Therefore, the Mann-Whitney U test was used to compare differences between these variables and long-term patient outcome. The significance threshold was set at ($p < .05$). This analysis measured the observed association between the patient outcome and continuous deviation of CPP from calculated CPPopt, known as ΔCPPopt(t) defined in equation (12). CPPopt(t) and PRx(t) values were also recalculated and analyzed for associations with patient outcomes. The difference between the real-time CPP and the optimal CPP is defined as:

$$\Delta CPPopt(t) = CPP(t) - CPPopt(t) \tag{12}$$

Full 2-hour episodes containing the most negative value of min(ΔCPPopt(t)) were selected along with the corresponding PRx(t) value for each patient. PRx values were calculated between both the minimum of ΔCPPopt(t) and GOS, and PRx(t) at the minimum of ΔCPPopt(t) and GOS. A critical event was defined as any period of time in which the PRx value was greater than 0.25 for all CPP values within the time window. It was assumed that critical event windows, where PRx > 0.25 for the entire window, are positively associated with fatal outcomes. This assumption was based off several studies which have demonstrated that TBI outcomes are more positively associated with critical events of CA impairments than the averaged PRx or CPPopt value [6, 16, 17]. Therefore, as outcome-related factors, the most critical 2-hour windows were selected. This enabled the use of these two variables to be used as additional parameters to indirectly test the model's efficiency. The set of ΔCPP(t) minimum values and corresponding PRx(t) values were calculated when all monitoring

episodes were included for calculation (without ML model), when episodes were selected by a physician (training data for ML model), and when informative episodes were predicted by ML.

3. Results

The main aim of this research was to develop and validate a ML algorithm to identify individual CPPopt values for TBI patients using only informative data. This chapter presents the results of the proposed algorithm, as well as analysis of performance parameters, linear regression, and the impact of adding STD values as an input. The results will focus on the accuracy of the ML algorithm to correctly classify patient episodes as 'informative' or 'non-informative' and its ability to detect individual CPPopt values in a shortened time window of 20-30 minutes.

3.1. Machine Learning Model Comparison

The SVM method (Acc = 68.8%) yielded significantly better results compared to the ANN method (Acc = 60.8%) in classification of 'informative' and 'non-informative' episodes. Therefore, the results of the ANN method have not been included and this chapter will focus instead on the SVM method.

3.2. Statistical Results

The application of the developed ML algorithm provided an increase in classification accuracy by 4.5% in detecting 'informative' and 'non-informative' patient episodes (from 77.58% to 82.1%). Further accuracy improvements were observed in detecting the LLCA and ULCA in CPP (21% increase), ABP (20% increase), ICP (6% increase), Critical CA (17.41% increase), and Intact CA (16.78%). The change in classification accuracy before and after the application of the developed ML algorithm are illustrated in **Fig. 10.**

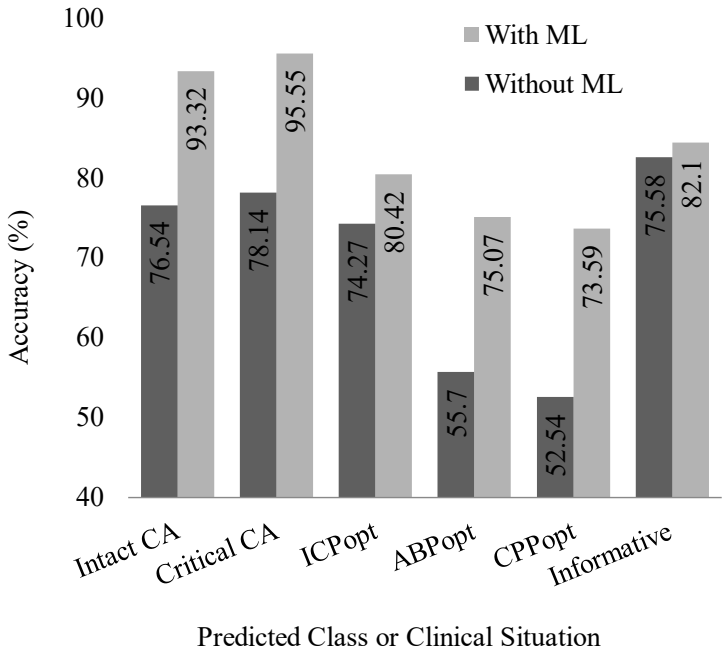

Fig. 10. Change in performance accuracy with the application of ML algorithm

The sensitivity and specificity of the developed ML algorithm in classifying 'informative' from 'non-informative' episodes are 0.364 and 0.954, respectively. In the detection of LLCA and ULCA, the highest sensitivity and specificity was identified in classifying patient episodes as 'Critical, requiring

immediate treatment intervention' (Se = 0.978, Sp = 0.911). The full results of the statistical analysis are presented in **Table 5.**

Table 5. Statistical analysis results

Predicted class or clinical situation	Acc	Acc (ML)	Se	Sp
Informative/Non-informative episode prediction	0.7558	0.821	0.3640	0.9540
1. CPP-based therapy is necessary	0.5254	0.7359	0.7721	0.6966
2. ABP-based therapy is necessary	0.5570	0.7507	0.8479	0.6189
3. ICP-based therapy is necessary	0.7427	0.8042	0.9742	0.3041
4. Critical CA	0.7814	0.9555	0.9717	0.9106
5. Intact CA	0.7654	0.9332	0.9562	0.8333

3.3. Correlation Results

Linear regression analysis was performed to determine associations between the dependent variable (patient outcome using GOS) and independent variables (the minimum of ΔCPPopt(t) and associated PRx(t) over the 2-hour monitoring window). The set of minimum values of ΔCPPopt(t) and the corresponding PRx(t) values were calculated in the cases when ML was not used, when the ML training data was used, and when the developed ML algorithm was used to classify informative episodes. No difference in associations were found using the developed ML algorithm and using the ML training data in comparison to without the use of any ML. When using the set of minimum ΔCPPopt values over the monitoring window as the outcome predicting factor, correlation coefficients were determined as r = .44 (without the use of ML) compared to r = .44 (using the ML training data) and r = .47 (using the developed ML algorithm). When using the set of PRx values over the monitoring as the outcome predicting factor, correlation coefficients were calculated as r = -.37 (without the use of ML) to r = -.46 (using the ML training data) and r = -44 (using the developed ML algorithm). Correlation coefficients when using the developed ML algorithm (ΔCPPopt r = .47, PRx r = -.44) have no significant difference from those calculated using the ML training data (ΔCPPopt r = .48, PRx r = -.46, $p < 0.05$). Plotted linear regression lines are presented in **Fig. 11** and **Fig. 12** showing positive and negative associations, respectively. All methods for calculating linear regression associations between ΔCPPopt to patient outcome refer to an averaged ΔCPPopt value.

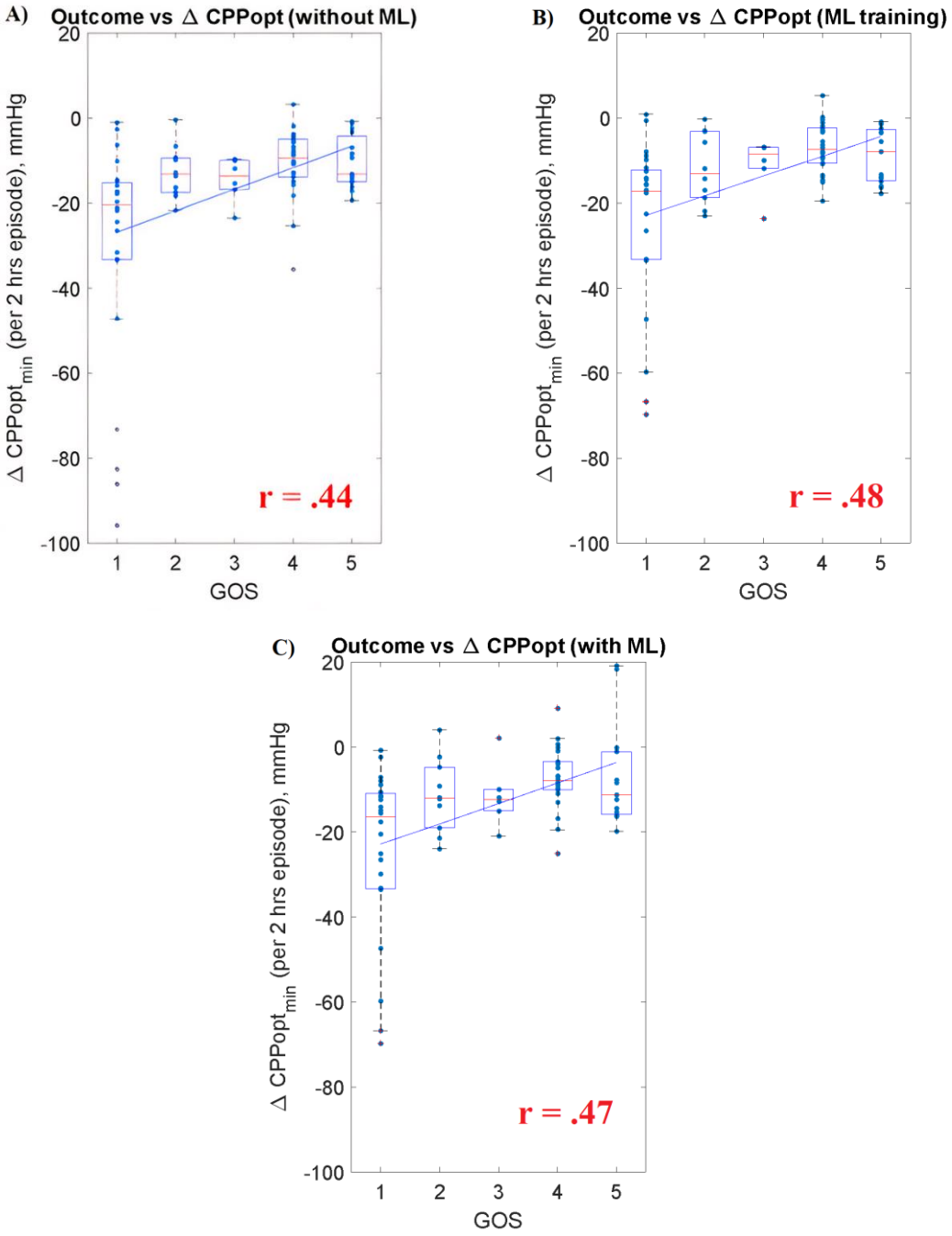

Fig. 11. Regression Analysis- Outcome vs CPPopt

Associations of patient outcome to the minimum ΔCPPopt values over the 2-hour monitoring window. Correlation coefficients were calculated as: A) when no ML was used (r = .44), B) when using the ML training data (r = .48), and C) through using the developed ML algorithm (r = .47).

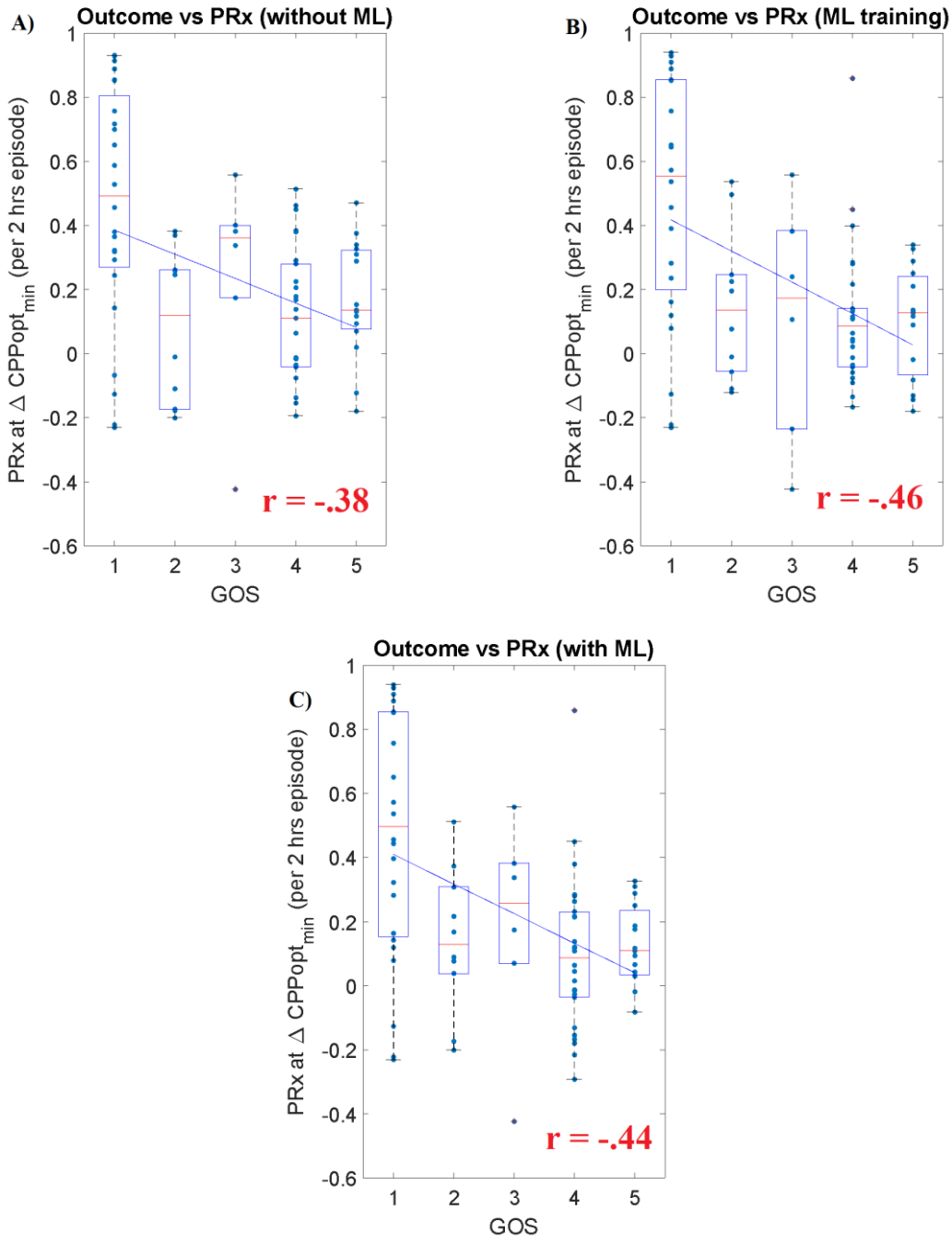

Fig. 12. Regression Analysis- Outcome vs PRx

Associations of patient outcome to the PRx values calculated from the set of minimum ΔCPPopt values over the entire 2-hour monitoring window. Correlation coefficients were calculated as: A) when ML is not used (r = -.38), B) when using the ML training data (r = -.46), and C) when using the developed ML algorithm (r = -.44).

3.4. Standard Deviation Results

Standard deviation ratios of ABP and ICP filtered with 1, 2, 3 and 4 minute moving average filters to non-filtered STD all showed significant different between groups with $p <<< 0.5$. The determined normalized STD ratios between ABP 'informative' and 'non-informative' episodes using the different moving average filter window times are illustrated in **Fig. 13**. The STD ratios between ICP

'informative' and 'non-informative' episodes using the different moving average filter window times are illustrated in **Fig. 14**. 'Non-informative' episodes are group 0, 'informative' episodes as group 1.

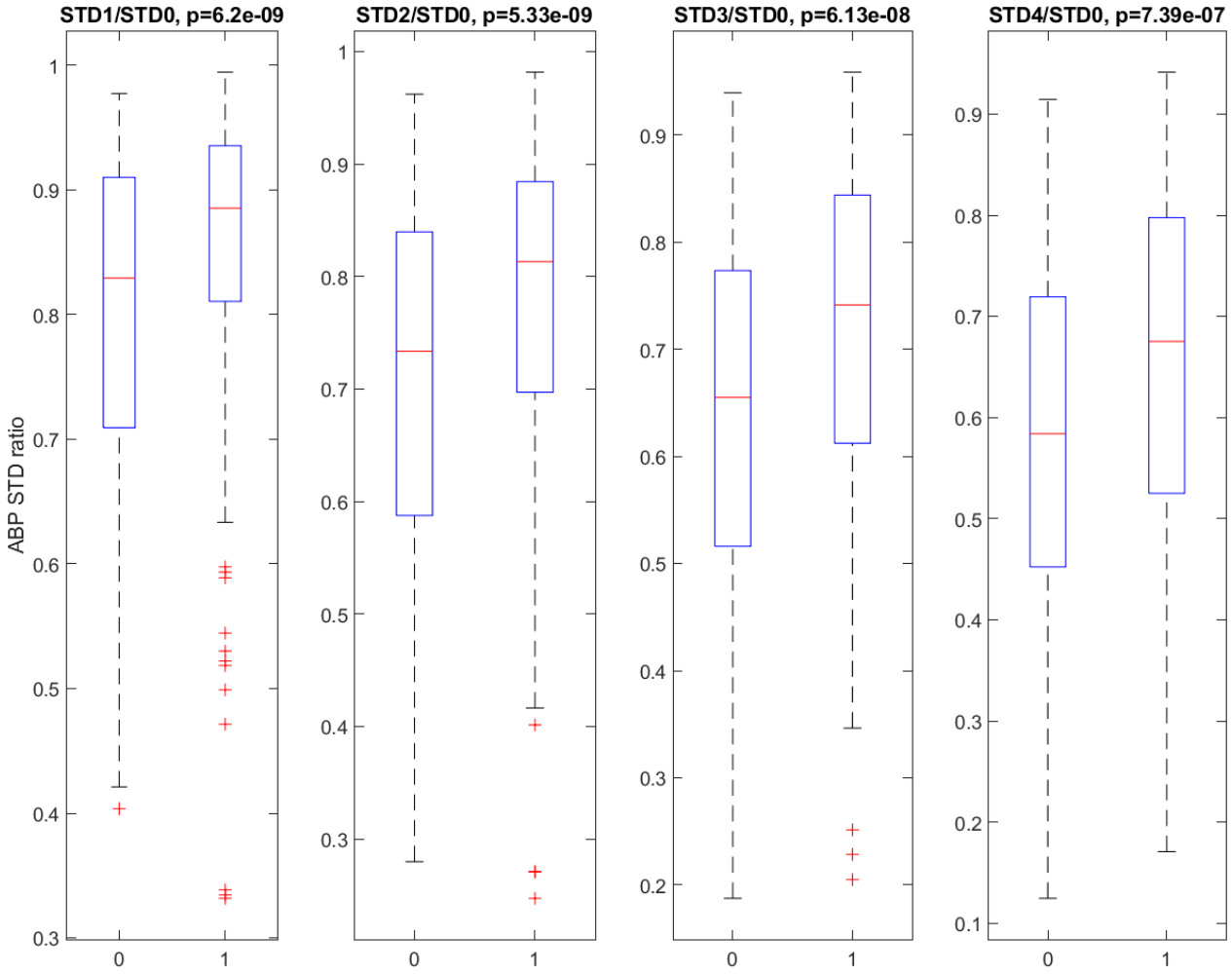

Fig. 13. Statistically significant differences of normalized STD ratios between 'informative' and 'non-informative' patient ICP monitoring episodes using 1-, 2-, 3- and 4-minute moving average filters. (0 = non-informative, 1 = informative).

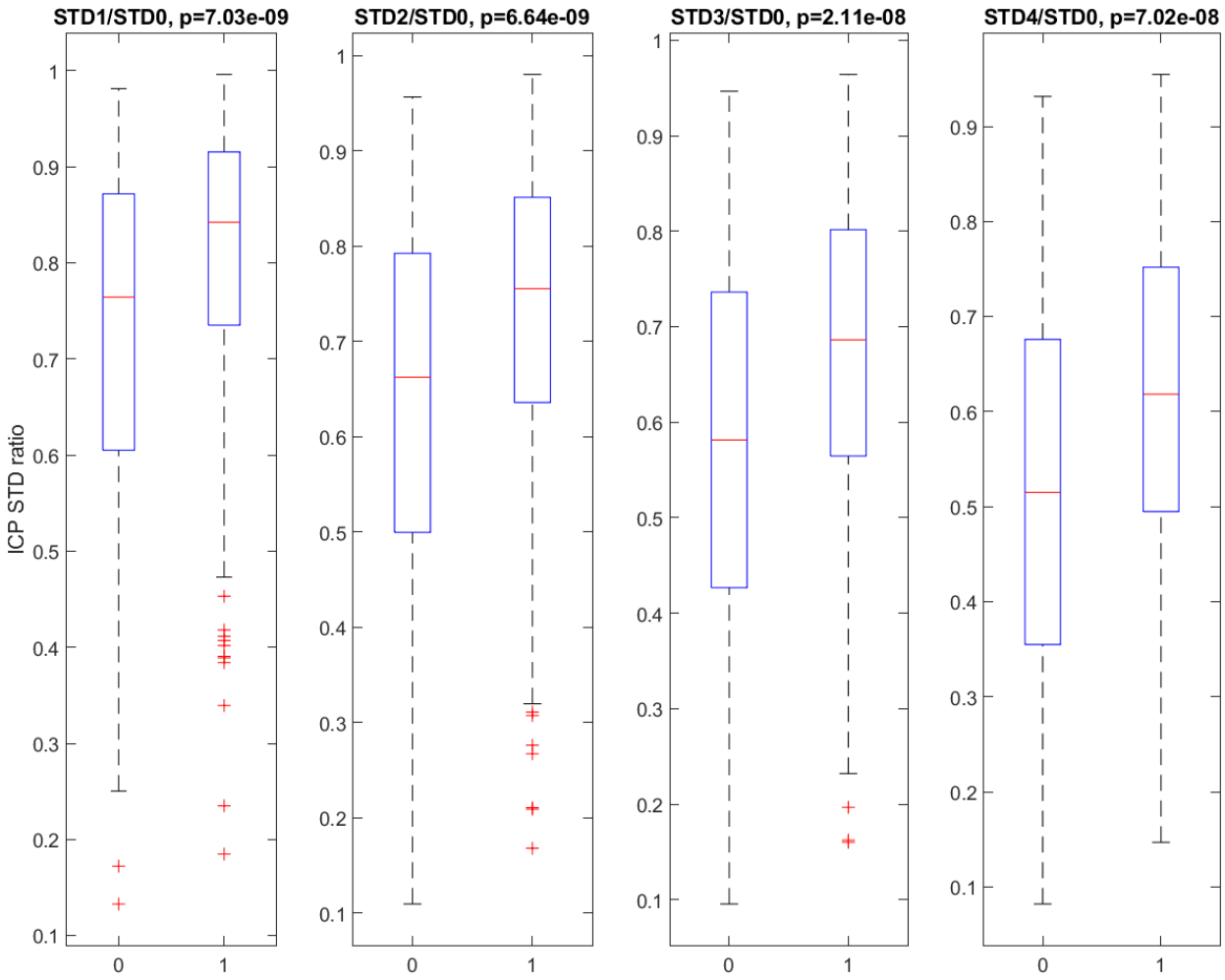

Fig. 14. Statistically significant differences of normalized STD ratios between 'informative' and 'non-informative' patient ICP monitoring episodes using 1-, 2-, 3- and 4-minute moving average filters. (0 = non-informative, 1 = informative).

3.5. CPPopt Identification

The developed ML algorithm was able to successfully identify individual patient CPPopt values in 'informative' episodes under 30-minutes where CPPopt was previously unidentifiable. Examples of the developed ML algorithm's CPPopt range values of different patient monitoring episodes are presented in **Fig. 15** and **Fig. 16**. Additional examples of patient episodes and comparisons of approximations before and after application of the developed ML are presented in **Appendix 1.** These examples illustrate that patient episodes containing informative ABP(t) and ICP(t) data under 30 minutes are sufficient to identify individual patient CPPopt values. In the graph, n.d. denotes not determined.

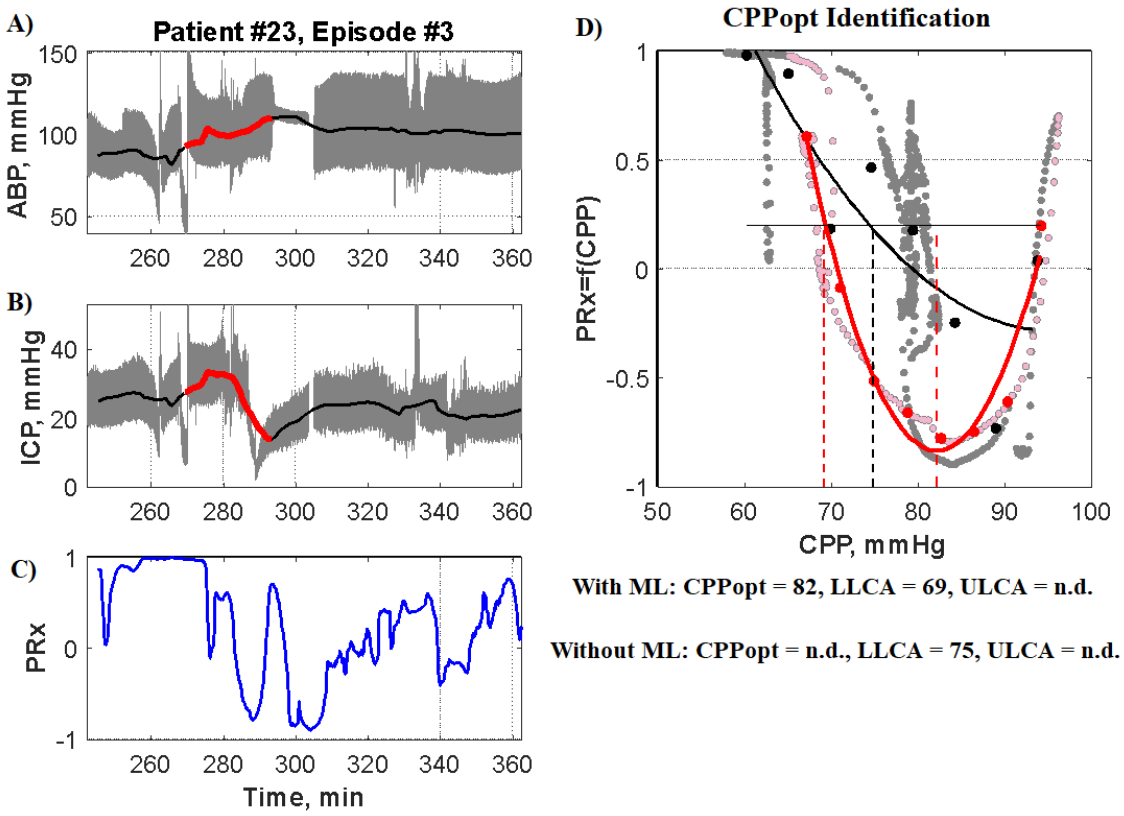

Fig. 15. Patient 23, Episode 3

Patient 23's episode 3 of 2-hour monitoring data after the application of the developed ML algorithm. A) and B) illustrate which episode out of the 2-hour monitoring window was selected as informative data by the developed ML algorithm, graphed in ABP and ICP, respectively. C) presents the calculated PRx value at each time using the associated values from the ABP and ICP graphs over the entire 2-hour time window. D) presents the graph of CPP vs PRx. The patient's individual CPPopt range approximations according to ML are illustrated by the red line (CPPopt = 82 mmHg, LLCA = 69 mmHg, and ULCA = n.d.) while values without ML are illustrated by the black line (CPPopt = n.d., LLCA = 75 mmHg, and ULCA = n.d.). In this example, the developed ML algorithm was able to identify the patient's individual CPPopt value (82 mmHg) when it could not be determined prior. Additionally, the ML-identified values for LLCA were decreased (from 75 mmHg to 69 mmHg).

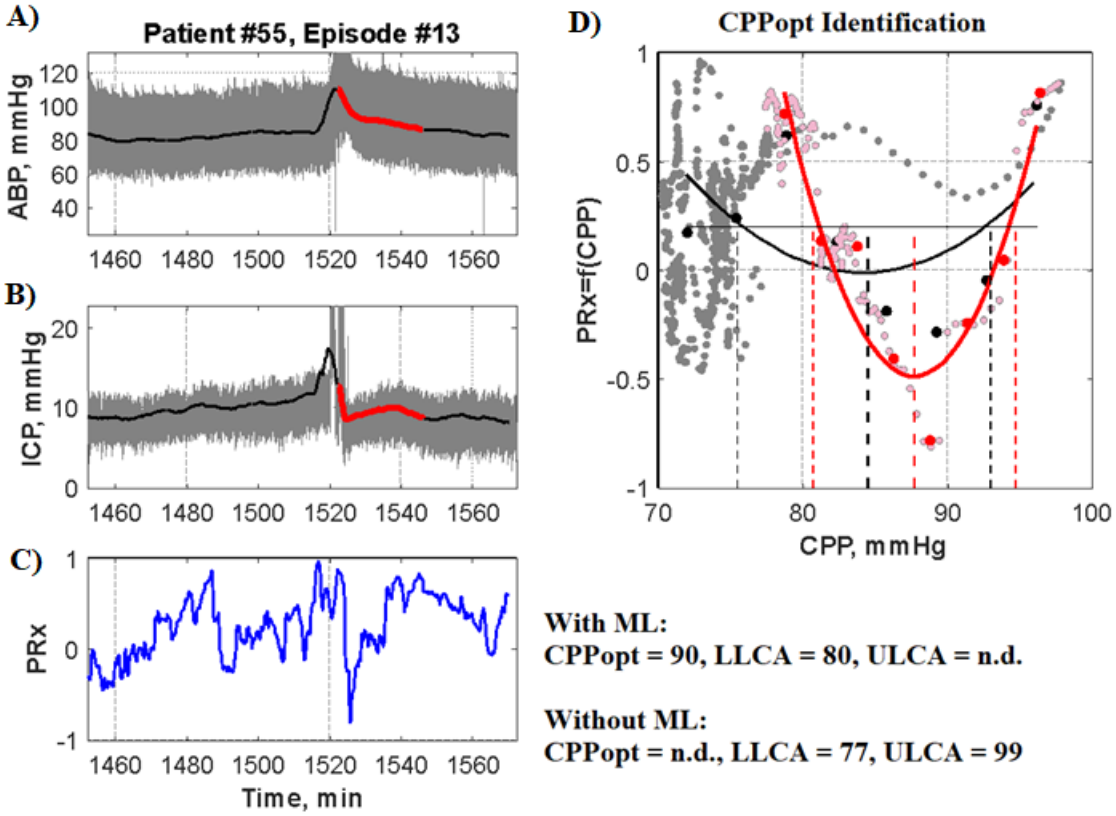

Fig. 16. Patient 55, Episode 13

Patient 55's episode 13 of 2-hour monitoring data after the application of the developed ML algorithm. A) and B) illustrate which episode out of the 2-hour monitoring window was selected as informative data by the developed ML algorithm, graphed in ABP and ICP, respectively. C) presents the calculated PRx value at each time using the associated values from the ABP and ICP graphs over the entire 2-hour time window. D) presents the graph of CPP vs PRx. The patient's individual CPPopt range approximations according to ML are illustrated by the red line (CPPopt = 90 mmHg, LLCA = 80 mmHg, and ULCA = n.d.), while values without ML are illustrated by the black line (CPPopt = n.d., LLCA = 77 mmHg, and ULCA = 99 mmHg). In this example, the application of our developed ML algorithm successfully identified the patient's individual CPPopt value (90 mmHg) when it was otherwise unidentifiable.

In summary of the presented results, preliminary comparisons of ML models illustrated that the SVM provided a 6% increase in identification of individual CPPopt values. The statistical analysis showed that the developed ML algorithm was able to identify individual CPPopt with 4.5% improved accuracy than without the use of ML. The regression analysis identified no difference in associations between patient outcome and calculated CPPopt values with without the ML algorithm. The STD results identify that the addition of their values was a key input for the developed ML algorithm to correctly classify informative and non-informative patient data segments. The developed ML algorithm illustrated several monitoring windows where the patient's induvial CPPopt was identified through recognition of 'informative' data.

4. Discussion

Keeping in mind that the aim of this research was to create a ML algorithm that could identify individual CPPopt values in TBI patients, there are five primary points of discussion for this study. First, the application of the developed ML algorithm provided a 4.5% improvement in the correct classification of 'informative' and 'non-informative' episodes (from 77.58% to 82.1%). In a clinical setting where patient stability is sensitive to minute changes in pressure and blood flow, this small improvement in detection accuracy and CPPopt identification can make a critical difference in improving outcomes for TBI patients. Yet, establishing the best treatment strategy for these patients based on optimal CPP, ABP, or ICP ranges can be difficult to determine when there are unknown influences distorting usable data. The largest improvement in performance accuracy upon application of the algorithm was observed in detecting the upper and lower limits of CA in CPP (21% increase) and ABP (20% increase) and thereby providing supplementary information to clinicians to aid decision-making.

Second, assessing the developed ML algorithm based solely on accuracy is not sufficient to evaluate performance. Sensitivity and specificity are measures that must be considered when determining whether a model has true applicability for medical treatment strategies. These parameters are prevalence-independent test characteristics, as their values are intrinsic to the ML model's performance. A higher sensitivity is fitting when the treatment strategy bears low risk. In these cases, doctors could take earlier treatment measures to potentially reduce mortality in TBI patients. In contrast, higher-risk treatment plans require increased specificity, as some patients may experience detrimental effects when specificity is not considered. Therefore, the applied ML algorithm must consider the trade-off between these two analysis parameters. The sensitivity and specificity of our ML model in predicting 'informative' from 'non-informative' episodes are 0.954 and 0.364, respectively. In this study, the high sensitivity value indicates that the developed ML model has done a successful job of predicting 'informative' episodes. The low specificity indicates that the model will incorrectly predict episodes as 'informative' when they are indeed 'non-informative'. The application of this research to medical treatments could be critical for patient mortality, so it is reasonable to be on the cautious side and allow more false positive predictions over false negative predictions. However, the developed ML algorithm's low specificity is noteworthy in isolating best performance, the study observed the highest sensitivity and specificity values for predicting clinical scenarios in the class 'Critical CA: requiring immediate treatment intervention', which indicates that the developed ML algorithm is most easily able to identify the lower and upper bounds of CA when the patient is in a critical state.

Third, linear regression analysis indicated a minimal change in association using the developed ML algorithm when comparing values of ΔCPPopt(t) and PRx(t) to long-term patient outcomes. This is further illustrated by the calculated correlation coefficients with model parameters to TBI patient outcomes from r = .44 (without ML) to r = .47 (with ML) when using min(ΔCPPopt), and from r = -.37 (without ML) to r = -.46 (with ML) when using PRx as an outcome predicting factor. The estimated corrected temporal ΔCPPopt values did not change drastically compared to averaged ΔCPPopt value and therefore, the results presented from the regression analysis approximation cannot directly prove added value of the ML algorithm. As the PRx is a global index providing an averaged index of all areas of the brain, it does not identify regions that might require adjusted CPPopt values. Therefore, while the regression analysis illustrates that the application of the developed ML algorithm

does not disturb identified CPPopt values, it does not directly support the application of ML in improving long-term patient outcomes.

The inclusion of the normalized STD ratios of ABP and ICP using moving average time filter windows were identified as key inputs that improved detection accuracy for 'informative' and 'non-informative' episodes. Specifically, using the 2-minute moving average time window filter resulted in the most statistically significant difference between groups in both ABP ($p = 5.33e{-9}$) and ICP ($p = 6.64e{-9}$) data. However, we expected that the inclusion of the calculated TFA gain and coherence would also increase the accuracy of the ML algorithm's 'informative' episode detection; yet the results indicate that this expectation was incorrect.

Finally, the most distinguished finding from this research is that individual CPPopt values were able to be identified within a time window shorter than 30 minutes, in contrast to the typical 4-hour window used in most PRx and CPP identification algorithms [11, 43]. Providing treatment within the first hour of patient admission to the ICU is critical for long-term patient outcomes [17], therefore this finding could drastically accelerate TBI patient treatment leading to improved outcomes. Examples of this are illustrated in **Fig. 15** and **Fig. 16**, where the patient ICP and ABP monitoring data contains enough informative information to identify individual CPPopt values within a 24-minute episode.

4.1. Limitations

This study was based on a series of assumptions and had a few noteworthy limitations. The key assumption in this study was that CPP-targeted management and treatment could be limited by numerous factors including anesthesia, changes in ICP and ABP, noisy signals, patient movement and artifacts. The second assumption was that an ML-based tool could assist physicians in deciding patient treatment pathways in these more complex scenarios with multiple influential factors such ICP and ABP data signal disturbances. The final assumption was that the accuracy of individual CPPopt value identification could be improved by eliminating artifacts and other non-informative data from the calculations.

The first limitation to highlight is that both PRx and CPPopt have never been subjected to prospective clinical trials. Therefore, their strength is only supported by retrospective analysis and a small number of pilot studies with low sample sizes. Retrospective studies can only determine association and not causation; and are subject to other risk factors that have not yet been identified. These limitations emphasize the need for further prospective studies to validate the use of machine learning algorithms in the identification of CPPopt values for TBI patients and related clinical applications.

Different forms of bias are important to identify as their influences can distort research results, lead to unnecessary costs, lower both the validity and reliability of research, and, given the critical nature of this study, risk a patient's life. The second notable limitation in this study is in the classification methodology for 'informative' and 'non-informative' episodes. This task was performed by medical physicists from the Lithuania University of Health Science and Vilnius University Hospital Clinic who are experienced in individual CPPopt-targeted treatments. However, the classification was made from their subjective opinion of what was deemed a critical informative feature, and a small number of episodes provided no clear distinguishable features. In some cases, the assignment of episodes as either 'informative' or 'non-informative' did not change individual CPPopt value identification. In other cases, when CA was either completely intact or impaired, the assignment of episodes to a

specific class was unclear and they were therefore annotated as ‘non-informative’ by default. These variations in the classification of episodes could influence the identified CPPopt values. For future research, designing a more consistent and unbiased method of episode classification would add reliability and validity to the study.

Third, a significant limitation that was not alleviated by the application of the developed ML algorithm is the requirement of informative ABP and ICP slow waves to calculate PRx and CPPopt values. When ABP and ICP signals are absent, slow waves must be artificially generated. There are several commonly used methods to generate slow waves in a clinical setting, but to calculate CPPopt and PRx values, the method must be performed repetitively every 1–2 minutes over a continuous monitoring window. The identified best method to accomplish this in a fragile clinical setting is called the Head-Up Tilt, which requires the subject to lie on a bed as the examiner adjusts the bed’s position for a set period [56]. Adjusting the head above or below the heart at specific degrees can cause a cerebrovascular response as the body adjusts to changing ICP. All hospitals have the capability to adjust a patient’s head tilt using electronic adjusters on the bed, making Head-Up tilt ideal to generate artificial slow waves when they are not readily present [50].

Finally, this study uses a relatively small sample size for ML validation (n = 84 patients, accounting for 11,230 patient episodes). This small size increases the likelihood of a Type II error, failing to observe a difference when there is one, potentially skewing the results, as well as introducing different forms of ML bias. Biases in ML algorithms are quite common when the amount of training data is insufficient and does not accurately represent the whole population. This can lead to poor performance of the algorithm on groups that were underrepresented in the initial training data. Given the consequences of an incorrect treatment for a TBI patient, this further emphasizes the need for research using larger sample sizes to better represent the diverse range of TBI patients and create more substantial databases that can be used to build improved ML algorithms. Taken together, these points emphasize the need for further research in this area to help mitigate assumptions, limitations, and challenges in the application of ML to identify individual CPPopt values.

4.2. Future Research

Further prospective clinical research with larger sample sizes and more reliable classification methods are needed to improve performance and reliability of the use ML-based algorithms in the determination of individual CPPopt values. This would contribute to the availability of larger databases that could be used to improve other ML classification models used in TBI research. Future research should explore integrating ML algorithms into current real-time bedside CA monitoring methods such as ICM+ Cambridge Software [52] with a goal to accelerate patient diagnosis and treatment.

Conclusions

1. The analysis software tool developed to create a database for this research can be used effectively for illustration, analysis, and annotation of continuous multimodal physiological patient data into ‘informative’ and ‘non-informative’ groups. This classification is based on the identification of specific informative features from patient ABP(t) and ICP(t) slow-wave forms. The resulting dataset from this tool comprised a database containing 20–30 minute annotated patient episodes, which can be utilized to train future machine learning algorithms. An additional feature of the developed analysis software tool is the ability to classify certain clinical situations and recommend treatments, such as CPP-based, ABP-based, and ICP-based management.

2. The developed machine learning algorithm can classify ‘informative’ and ‘non-informative’ patient monitoring data episodes with a 4.5% increase in accuracy based on feature recognition of critical events and the comparison of standard deviation values in patient ABP(t) and ICP(t) slow-wave forms. With the selected ‘informative’ episodes, the developed algorithm can identify individual patient CPPopt values and/or the lower and upper limits of CA. Additionally, the developed algorithm can identify certain clinical situations and associated recommended treatments with increased accuracy compared to traditional methods. It was 21% more accurate when using CPP, 20% for ABP, and 6% for ICP-based managements.

3. Individualized patient CPPopt values can be identified in continuous monitoring episodes that are 20–30 minutes in length when these episodes contain informative ABP(t) and ICP(t) slow-wave data. This finding suggests that CPPopt values can be identified 10 times faster than the typical technologies used in the ICU at the time of the study, which require a 4-hour continuous data monitoring window. This advancement has the potential to expedite TBI patient treatment, improve patient outcomes and indirectly reduce mortality rates.

List of References

1. MAAS, Andrew I.R. et al. Collaborative European NeuroTrauma Effectiveness Research in Traumatic Brain Injury (CENTER-TBI). *Neurosurgery* [online]. January 2015. **76**(1), 67–80. [Accessed 8 February 2021]. Available from: https://doi.org/10.1227/NEU.0000000000000575

2. CARNEY, Nancy et al. Guidelines for the Management of Severe Traumatic Brain Injury, Fourth Edition. *Neurosurgery* [online]. 1 January 2017. **80**(1), 6–15. [Accessed 16 March 2021]. Available from: 10.1227/NEU.0000000000001432

3. STEINER, Luzius A. et al. Continuous monitoring of cerebrovascular pressure reactivity allows determination of optimal cerebral perfusion pressure in patients with traumatic brain injury. *Critical Care Medicine* [online]. April 2002. **30**(4), 733–738. [Accessed 16 April 2021]. Available from: 10.1097/00003246-200204000-00002

4. LAZARIDIS, Christos et al. Optimal cerebral perfusion pressure: are we ready for it? *Neurological Research* [online]. 12 March 2013. **35**(2), 138–148. [Accessed 1 February 2021]. Available from: 10.1179/1743132812Y.0000000150

5. LIU, Xiuyun et al. Assessment of cerebral autoregulation indices – a modelling perspective. *Scientific Reports*. 15 December 2020. **10**(1), . DOI 10.1038/s41598-020-66346-6.

6. PETKUS, Vytautas et al. Benefit on optimal cerebral perfusion pressure targeted treatment for traumatic brain injury patients. *Journal of Critical Care* [online]. October 2017. **41**49–55. [Accessed 16 March 2021]. Available from: 10.1016/j.jcrc.2017.04.029

7. RIEMANN, Lennart et al. Low-resolution pressure reactivity index and its derived optimal cerebral perfusion pressure in adult traumatic brain injury: a CENTER-TBI study. *Critical Care* [online]. 26 December 2020. **24**(1), 266–267. [Accessed 7 April 2021]. Available from: 10.1186/s13054-020-02974-8

8. DEPREITERE, Bart et al. Pressure autoregulation monitoring and cerebral perfusion pressure target recommendation in patients with severe traumatic brain injury based on minute-by-minute monitoring data. *Journal of Neurosurgery* [online]. June 2014. **120**(6), 1451–1457. [Accessed 15 January 2021]. Available from: 10.3171/2014.3.JNS131500

9. ARIES, Marcel J. H. et al. Continuous determination of optimal cerebral perfusion pressure in traumatic brain injury*. *Critical Care Medicine* [online]. August 2012. **40**(8), 2456–2463. [Accessed 3 April 2021]. Available from: 10.1097/CCM.0b013e3182514eb6

10. RABOEL, P. H. et al. Intracranial Pressure Monitoring: Invasive versus Non-Invasive Methods—A Review. *Critical Care Research and Practice* [online]. 2012. **2012**950393–950394. [Accessed 23 February 2021]. Available from: 10.1155/2012/950393

11. DIAS, Celeste et al. Optimal Cerebral Perfusion Pressure Management at Bedside: A Single-Center Pilot Study. *Neurocritical Care* [online]. 8 August 2015. **23**(1), 92–201. [Accessed 4 January 2021]. Available from: 10.1007/s12028-014-0103-8

12. JAEGER, Matthias et al. Effects of cerebrovascular pressure reactivity-guided optimization of cerebral perfusion pressure on brain tissue oxygenation after traumatic brain injury*. *Critical Care Medicine* [online]. May 2010. **38**(5), 1343–1347. [Accessed 2 March 2021]. Available from: 10.1097/CCM.0b013e3181d45530

13. SLUPE, Andrew M and KIRSCH, Jeffrey R. Effects of anesthesia on cerebral blood flow, metabolism, and neuroprotection. *Journal of Cerebral Blood Flow & Metabolism* [online]. 16 December 2018. **38**(12), 2192–2208. [Accessed 27 February 2021]. Available from: 10.1177/0271678X18789273

14. BEDFORTH, N.M. et al. Effects of desflurane on cerebral autoregulation. *British Journal of Anaesthesia* [online]. August 2001. **87**(2), 193–197. [Accessed 22 March 2021]. Available from: 10.1093/bja/87.2.193
15. WETTERVIK, Teodor Svedung et al. Autoregulatory or Fixed Cerebral Perfusion Pressure Targets in Traumatic Brain Injury: Determining Which Is Better in an Energy Metabolic Perspective. *Journal of Neurotrauma* [online]. 1 March 2021. [Accessed 8 March 2021]. Available from: 10.1089/neu.2020.7290
16. PETKUS, Vytautas et al. Optimal Cerebral Perfusion Pressure: Targeted Treatment for Severe Traumatic Brain Injury. *Journal of Neurotrauma* [online]. 15 January 2020. **37**(2), 389–396. [Accessed 11 December 2020]. Available from: 10.1089/neu.2019.6551
17. PREIKSAITIS, Aidanas et al. Association of Severe Traumatic Brain Injury Patient Outcomes with Duration of Cerebrovascular Autoregulation Impairment Events. *Neurosurgery* [online]. July 2016. **79**(1), 75–82. [Accessed 8 March 2021]. Available from: 10.1227/NEU.0000000000001192
18. DAG, Ali et al. Predicting heart transplantation outcomes through data analytics. *Decision Support Systems* [online]. February 2017. **94**. [Accessed 11 May 2021]. Available from: https://doi.org/10.1016/j.dss.2016.10.005
19. WALKER, William C. et al. Predicting Long-Term Global Outcome after Traumatic Brain Injury: Development of a Practical Prognostic Tool Using the Traumatic Brain Injury Model Systems National Database. *Journal of Neurotrauma* [online]. 15 July 2018. **35**(14), 587–595. [Accessed 9 May 2021]. Available from: 10.1089/neu.2017.5359
20. HALE, Andrew T. et al. Machine-learning analysis outperforms conventional statistical models and CT classification systems in predicting 6-month outcomes in pediatric patients sustaining traumatic brain injury. *Neurosurgical Focus* [online]. November 2018. **45**(5), E2–E3. [Accessed 11 May 2021]. DOI +. Available from: 10.3171/2018.8.FOCUS17773
21. FENG, Jin-zhou et al. Comparison between logistic regression and machine learning algorithms on survival prediction of traumatic brain injuries. *Journal of Critical Care* [online]. December 2019. **54**110–116. [Accessed 4 April 2021]. Available from: 10.1016/j.jcrc.2019.08.010
22. LIU, Xiuyun et al. Monitoring of Optimal Cerebral Perfusion Pressure in Traumatic Brain Injured Patients Using a Multi-Window Weighting Algorithm. *Journal of Neurotrauma* [online]. 15 November 2017. **34**(22), 3081–3088. [Accessed 16 February 2021]. Available from: 10.1089/neu.2017.5003
23. VISHWANATH, Manoj et al. Investigation of Machine Learning Approaches for Traumatic Brain Injury Classification via EEG Assessment in Mice. *Sensors* [online]. 4 April 2020. **20**(7), 2027–2029. [Accessed 26 March 2021]. Available from: 10.3390/s20072027
24. RAU, Cheng-Shyuan et al. Mortality prediction in patients with isolated moderate and severe traumatic brain injury using machine learning models. *PLOS ONE* [online]. 9 November 2018. **13**(11), 1–12. [Accessed 16 February 2021]. Available from: 10.1371/journal.pone.0207192
25. ABUJABER, Ahmad et al. Prediction of in-hospital mortality in patients with post traumatic brain injury using National Trauma Registry and Machine Learning Approach. *Scandinavian Journal of Trauma, Resuscitation and Emergency Medicine* [online]. 27 December 2020. **28**(1), . [Accessed 18 February 2021]. DOI 10.1186/s13049-020-00738-5. Available from: 10.1186/s13049-020-00738-5
26. GÜIZA, Fabian et al. Novel Methods to Predict Increased Intracranial Pressure During Intensive Care and Long-Term Neurologic Outcome After Traumatic Brain Injury. *Critical Care Medicine* [online]. February 2013. **41**(2), 554–564. [Accessed 13 January 2021]. Available from: 10.1097/CCM.0b013e3182742d0a

27. SILVERMAN, A. and Petersen, N.H. Physiology, Cerebral Autoregulation. In: *StatPearls* [online]. Treasure Island (FL): StatPearls Publishing, 2020. p. 465–477. [Accessed 11 December 2020]. Available from: https://www.ncbi.nlm.nih.gov/books/NBK553183/
28. TZENG, Y. C. and PANERAI, R. B. CrossTalk proposal: dynamic cerebral autoregulation should be quantified using spontaneous blood pressure fluctuations. *The Journal of Physiology* [online]. 1 January 2018. **596**(1), 545–559. [Accessed 3 March 2021]. Available from: 10.1113/JP273899
29. PANERAI, Ronney B. et al. Grading of Cerebral Dynamic Autoregulation from Spontaneous Fluctuations in Arterial Blood Pressure. *Stroke* [online]. November 1998. **29**(11), 2341–2346. [Accessed 16 March 2021]. Available from: 10.1161/01.STR.29.11.2341
30. LASSEN, Niels A. Cerebral Blood Flow and Oxygen Consumption in Man. *Physiological Reviews* [online]. 1 April 1959. **39**(2), 183–238. [Accessed 8 February 2021]. Available from: 10.1152/physrev.1959.39.2.183
31. ARMSTEAD, William M. Cerebral Blood Flow Autoregulation and Dysautoregulation. *Anesthesiology Clinics* [online]. September 2016. **34**(3), 465–477. [Accessed 26 March 2021]. Available from: 10.1016/j.anclin.2016.04.002
32. Brain Trauma Foundation. [online]. 2020. [Accessed 30 April 2021]. Available from: https://www.braintrauma.org/faq
33. TOTH, Peter et al. Traumatic brain injury-induced autoregulatory dysfunction and spreading depression-related neurovascular uncoupling: Pathomechanisms, perspectives, and therapeutic implications. *American Journal of Physiology-Heart and Circulatory Physiology* [online]. 1 November 2016. **311**(5), 1118–1131. [Accessed 25 January 2021]. Available from: 10.1152/ajpheart.00267.2016
34. ZEILER, Frederick A. et al. Pressure Autoregulation Measurement Techniques in Adult Traumatic Brain Injury, Part II: A Scoping Review of Continuous Methods. *Journal of Neurotrauma* [online]. December 2017. **34**(23), 25–39. [Accessed 18 January 2021]. Available from: 10.1089/neu.2017.5086
35. PETKUS, Vytautas et al. Non-invasive Cerebrovascular Autoregulation Assessment Using the Volumetric Reactivity Index: Prospective Study. *Neurocritical Care* [online]. 27 February 2019. **30**(1), 42–50. [Accessed 27 January 2021]. Available from: 10.1007/s12028-018-0569-x
36. ESCH, Ben T. A. et al. Construction of a lower body negative pressure chamber. *Advances in Physiology Education* [online]. January 2007. **31**(1), 76–81. [Accessed 3 April 2021]. Available from: 10.1152/advan.00009.2006
37. LEMAIRE, J. J. et al. Slow pressure waves in the cranial enclosure. *Acta Neurochirurgica* [online]. March 2002. **144**(3), 243–254. [Accessed 10 November 2020]. Available from: 10.1007/s007010200032
38. CZOSNYKA, M. et al. Monitoring and interpretation of intracranial pressure after head injury. In: *Brain Edema XIII* [online]. Vienna: Springer-Verlag, [no date]. [Accessed 25 February 2021]. Available from: 10.1007/3-211-30714-1_26
39. DONNELLY, Joseph et al. Individualizing Thresholds of Cerebral Perfusion Pressure Using Estimated Limits of Autoregulation. *Critical Care Medicine* [online]. September 2017. **45**(9), 1464–1471. [Accessed 9 May 2021]. Available from: 10.1097/CCM.0000000000002575
40. NEEDHAM, Edward et al. Cerebral Perfusion Pressure Targets Individualized to Pressure-Reactivity Index in Moderate to Severe Traumatic Brain Injury: A Systematic Review. *Journal of Neurotrauma* [online]. March 2017. **34**(5), 963–997. [Accessed 1 April 2021]. Available from: 10.1089/neu.2016.4450

41. DONNELLY, J. et al. Pressure Reactivity-Based Optimal Cerebral Perfusion Pressure in a Traumatic Brain Injury Cohort. *Acta neurochirurgica Supplement* [online]. 2018. **126**(1), 209–212. [Accessed 10 December 2020]. Available from: 10.1007/978-3-319-65798-1_43
42. LANG, Erhard W. et al. Short pressure reactivity index versus long pressure reactivity index in the management of traumatic brain injury. *Journal of Neurosurgery* [online]. March 2015. **122**(3), 588–594. [Accessed 27 November 2020]. Available from: 10.3171/2014.10.JNS14602
43. BEQIRI, Erta et al. Feasibility of individualised severe traumatic brain injury management using an automated assessment of optimal cerebral perfusion pressure: The COGiTATE phase II study protocol. *BMJ Open* [online]. 20 September 2019. **9**(9), 30727–30728. [Accessed 19 April 2021]. Available from: 10.1136/bmjopen-2019-030727
44. OGAWA, Yojiro et al. Dexmedetomidine Weakens Dynamic Cerebral Autoregulation as Assessed by Transfer Function Analysis and the Thigh Cuff Method. *Anesthesiology* [online]. 1 October 2008. **109**(4), 642–650. [Accessed 18 March 2021]. Available from: 10.1097/ALN.0b013e3181862a33
45. ENDOH, Hiroshi et al. The Effects of Nicardipine on Dynamic Cerebral Autoregulation in Patients Anesthetized with Propofol and Fentanyl. *Anesthesia & Analgesia* [online]. September 2000. **91**(3), 642–646. [Accessed 10 November 2020]. Available from: 10.1097/00000539-200009000-00027
46. GÜIZA, Fabian et al. Continuous Optimal CPP Based on Minute-by-Minute Monitoring Data: A Study of a Pediatric Population. In: *Intracranial Pressure and Brain Monitoring XV* [online]. Supplement 122. Springer International Publishing, 2016. [Accessed 11 May 2021]. ISBN 978-3-319-22532-6, 978-3-319-22533-3. Available from: 10.1007/978-3-319-22533-3_38
47. RAJ, Rahul et al. Machine learning-based dynamic mortality prediction after traumatic brain injury. *Scientific Reports* [online]. 27 December 2019. **9**(1), :17672-17673. [Accessed 10 February 2021]. Available from: https://doi.org/10.1038/s41598-019-53889-6
48. HAN, J et al. Data mining: concepts and techniques. In: *In the Morgan Kaufmann Series in Data Management Systems* [online]. 3rd. San Francisco: Morgan Kaufmann Publishers Inc, 2012. p. 393–442. [Accessed 11 May 2021]. ISBN 9780123814791. Available from: https://doi.org/10.1016/B978-0-12-381479-1.00009-5.
49. ABUJABER, Ahmad et al. Prediction of in-hospital mortality in patients with post traumatic brain injury using National Trauma Registry and Machine Learning Approach. *Scandinavian Journal of Trauma, Resuscitation and Emergency Medicine* [online]. 27 December 2020. **28**(4), 1–6. [Accessed 14 February 2021]. Available from: https://doi.org/10.1227/NEU.0000000000000575
50. MUSHKUDIANI, Nino A. et al. A systematic review finds methodological improvements necessary for prognostic models in determining traumatic brain injury outcomes. *Journal of Clinical Epidemiology* [online]. April 2008. **61**(4), 331–343. [Accessed 11 May 2021]. Available from: 10.1016/j.jclinepi.2007.06.011
51. GRAVESTEIJN, Benjamin Y. et al. Machine learning algorithms performed no better than regression models for prognostication in traumatic brain injury. *Journal of Clinical Epidemiology* [online]. June 2020. **122**(1), 95–107. [Accessed 29 January 2021]. Available from: 10.1016/j.jclinepi.2020.03.005
52. MAREK CZOSNYKA and PETER SMIELEWSKI. *ICM+: software for on-line analysis of bedside monitoring data after severe head trauma*. 2020. Cambridge, England: Cambridge Enterprises.

53. R CORE TEAM. *R: A Language and Environment for Statistical Computing* [online]. 2020. Vienna, Austria: R Foundation for Statistical Computing. R2020. Available from: https://www.R-project.org/
54. KIRILL MÜLLER. *e1071 package: Misc Functions of the Department of Statistics, Probability Theory Group* [online]. 2020. 1.7-6. Available from: https://CRAN.R-project.org/package=e1071
55. VAN BEEK, Arenda HEA et al. Cerebral Autoregulation: An Overview of Current Concepts and Methodology with Special Focus on the Elderly. *Journal of Cerebral Blood Flow & Metabolism* [online]. 19 June 2008. **28**(6), 1071–1085. [Accessed 17 May 2021]. Available from: 10.1038/jcbfm.2008.13
56. TYMKO, Michael M. et al. Steady-state tilt has no effect on cerebrovascular CO2 reactivity in anterior and posterior cerebral circulations. *Experimental Physiology* [online]. 1 July 2015. **100**(7), 839–851. [Accessed 10 November 2020]. Available from: 10.1113/EP085084
57. CZOSNYKA, Marek et al. Continuous Assessment of the Cerebral Vasomotor Reactivity in Head Injury. *Neurosurgery* [online]. 1 July 1997. **41**(1), 11–17. [Accessed 3 April 2021]. Available from: 10.1097/00006123-199707000-00005

Appendices

Appendix 1. Machine Learning CPPopt Identification Examples

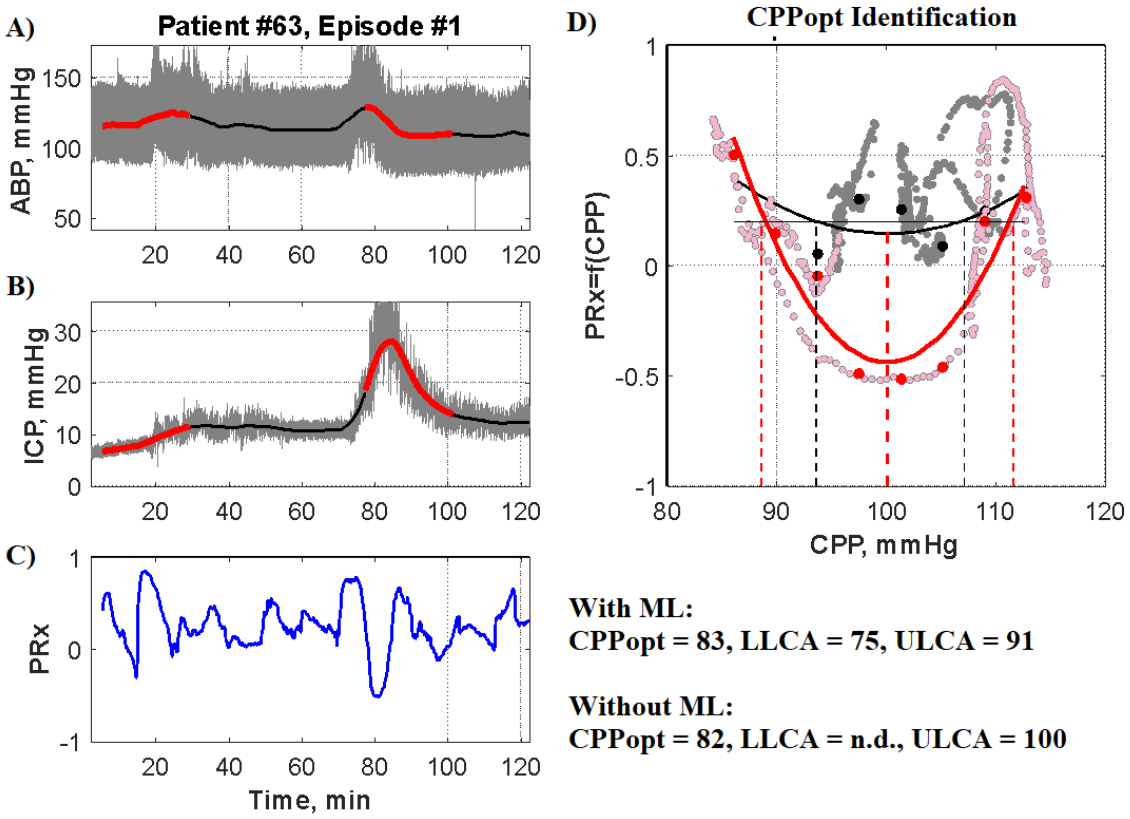

Fig. 17. Patient 63, Episode 1

Patient 63's episode 1 of 2-hour monitoring data. A) and B) illustrate which episode out of the 2-hour monitoring window was selected as informative data by the developed ML algorithm, graphed in ABP and ICP, respectively. C) presents the calculated PRx value at each time using the associated values from the ABP and ICP graphs over the entire 2-hour time window. D) presents the graph of CPP vs PRx. The patient's individual CPPopt range approximations according to ML are illustrated by the red line (CPPopt = 83 mmHg, LLCA = 75 mmHg, and ULCA = 91 mmHg), while values without ML are illustrated by the black line (CPPopt = 82 mmHg, LLCA = n.d. and ULCA = 100 mmHg). In this example, the developed ML algorithm was able to identify the patient's range of stable CA when it was otherwise unidentifiable. It also calculated CPPopt within these new bounds, which increased CPPopt from 82 mmHg to 83 mmHg.

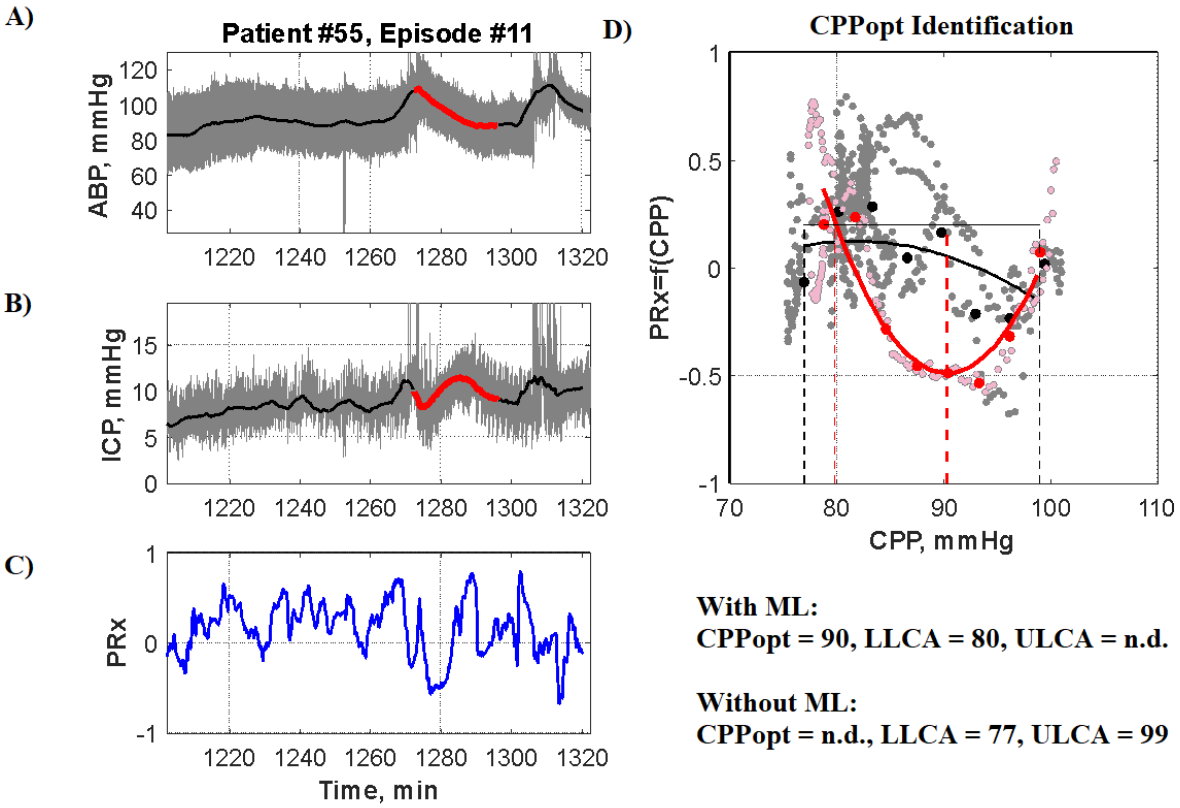

Fig. 18. Patient 55, Episode 11

Patient 55's episode 11 of 2-hour monitoring data. A) and B) illustrate which episode out of the 2-hour monitoring window was selected as informative data by the developed ML algorithm, graphed in ABP and ICP, respectively. C) presents the calculated PRx value at each time using the associated values from the ABP and ICP graphs over the entire 2-hour time window. D) presents the graph of CPP vs PRx. The patient's individual CPPopt range approximations according to ML are illustrated by the red line (CPPopt = 90 mmHg, LLCA = 80 mmHg, and ULCA = n.d.), while values without ML are illustrated by the black line (CPPopt = n.d., LLCA = 77 mmHg, and ULCA = 99 mmHg).

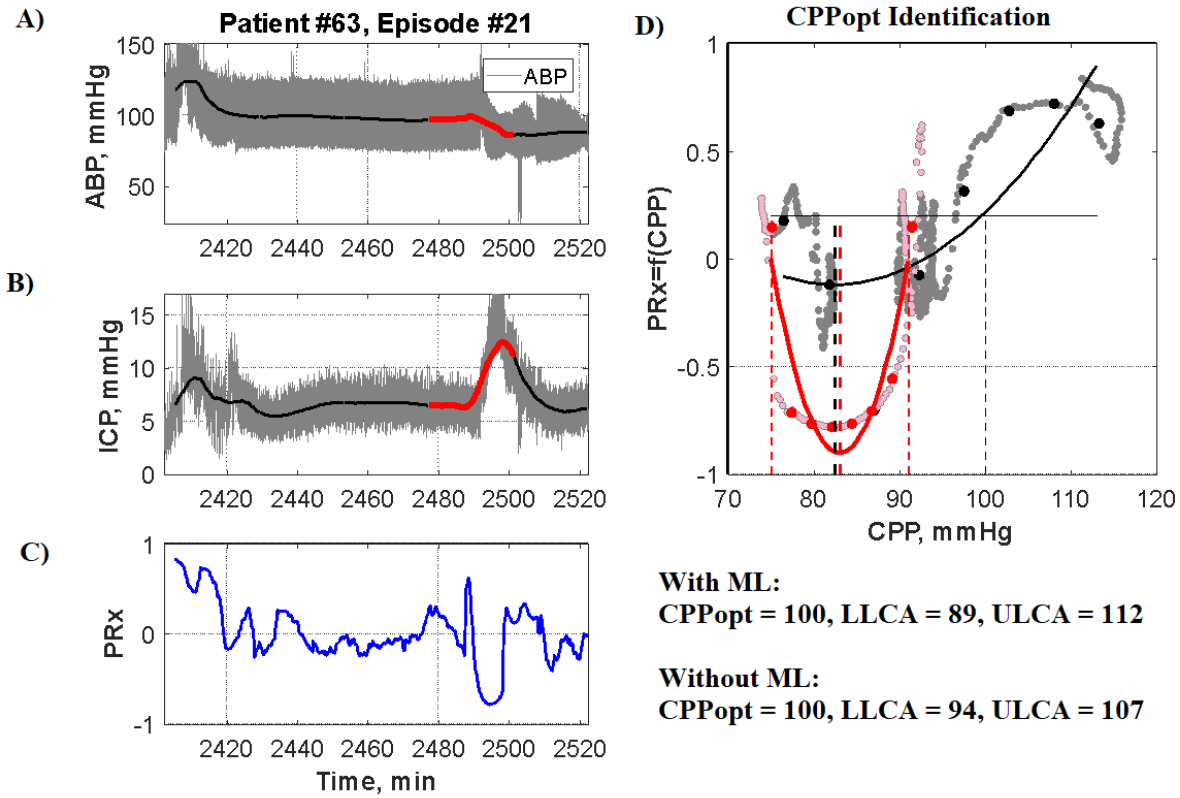

Fig. 19. Patient 63, Episode 21

Patient 63's episode1 1 of 2-hour monitoring data. A) and B) illustrate which episode out of the 2-hour monitoring window was selected as informative data by the developed ML algorithm, graphed in ABP and ICP, respectively. C) presents the calculated PRx value at each time using the associated values from the ABP and ICP graphs over the entire 2-hour time window. D) presents the graph of CPP vs PRx. The patient's individual CPPopt range approximations according to ML are illustrated by the red line (CPPopt = 100 mmHg, LLCA = 89 mmHg, and ULCA = 112 mmHg) while values without ML are illustrated by the black line (CPPopt =100 mmHg, LLCA = 94 mmHg, and ULCA = 107 mmHg). In this example, the defined lower and upper limits of CA have been expanded with the use of ML, but the individual's identified CPPopt value did not change.

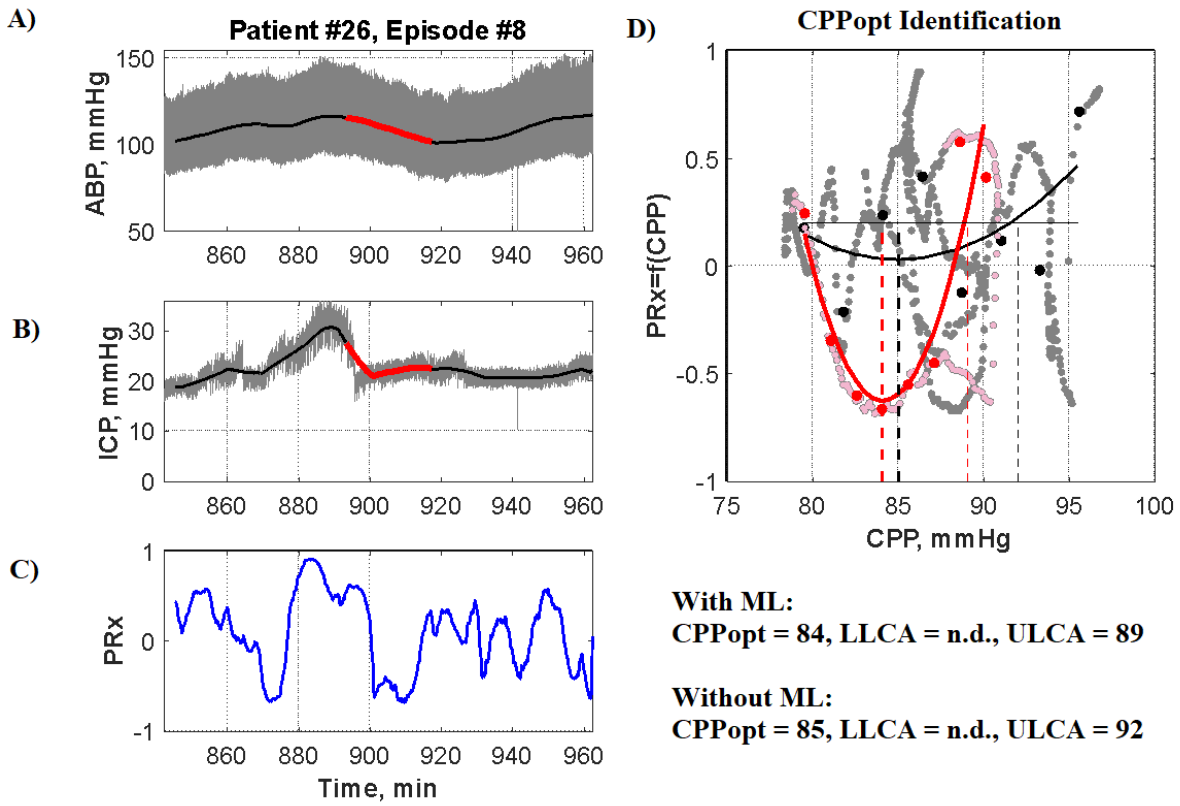

Fig. 20. Patient 26, Episode 8

Patient 26's episode 8 of monitoring window after the application of the ML algorithm. A) and B) illustrate which episode out of the 2-hour monitoring window was selected as informative data by the developed ML algorithm, graphed in ABP and ICP, respectively. C) presents the calculated PRx value at each time using the associated values from the ABP and ICP graphs over the entire 2-hour time window. D) presents the graph of CPP vs PRx. The patient's individual CPPopt range approximations according to ML are illustrated by the red line (CPPopt = 84 mmHg, LLCA = n.d., and ULCA = 89 mmHg), while values without ML are illustrated by the black line (CPPopt = 85 mmHg, LLCA = n.d., and ULCA = 92 mmHg). In this example, the application of ML has reduced the CPPopt value (from 84 mmHg to 83 mmHg) and lowered the ULCA value (from 92 mmHg to 89 mmHg).

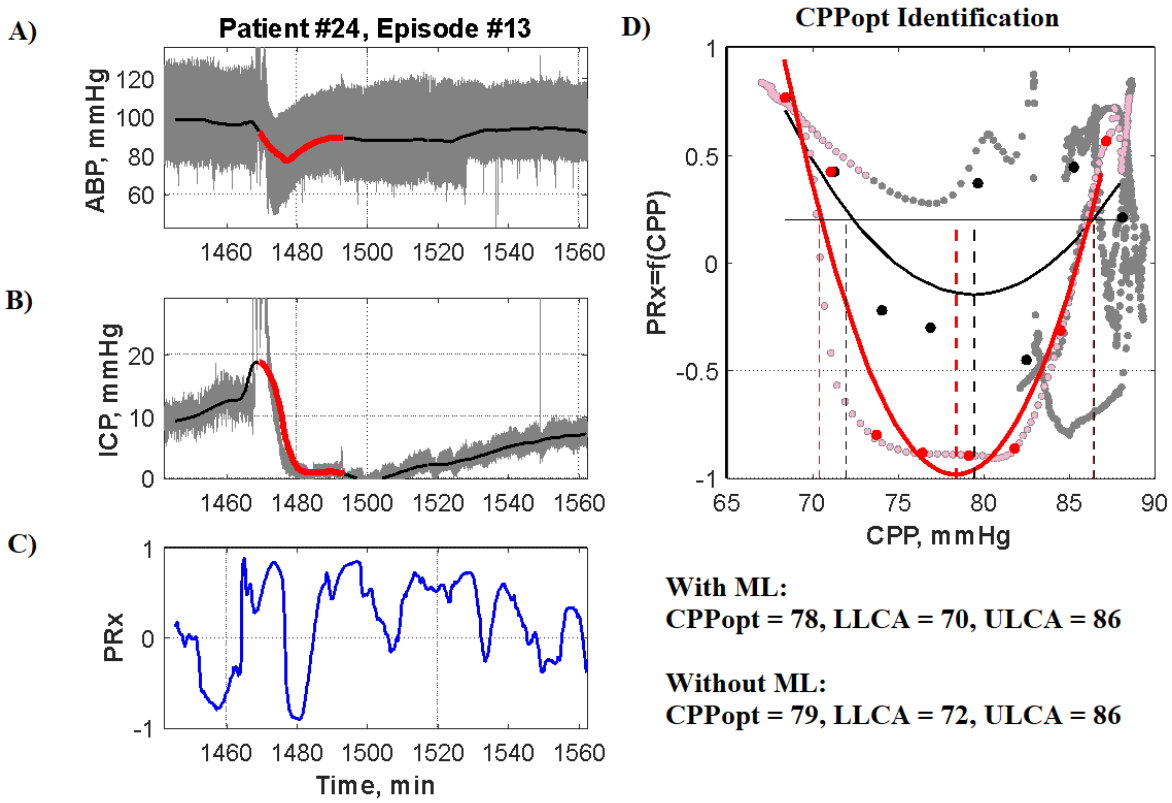

Fig. 21. Patient 24, Episode 13

Patient 24's episode 13 of the 2-hour monitoring window after the application of the developed ML algorithm. A) and B) illustrate which episode out of the 2-hour monitoring window was selected as informative data by the developed ML algorithm, graphed in ABP and ICP, respectively. C) presents the calculated PRx value at each time using the associated values from the ABP and ICP graphs over the entire 2-hour time window. D) presents the graph of CPP vs PRx. The patient's individual CPPopt range approximations according to ML are illustrated by the red line (CPPopt = 78 mmHg, LLCA = 70 mmHg, and ULCA = 86 mmHg) while values without ML are illustrated by the black line (CPPopt = 79 mmHg, LLCA = 72 mmHg, and ULCA = 86 mmHg). In this example, the application of ML has reduced the CPPopt value (from 79 mmHg to 78 mmHg) and lowered the LLCA value (from 72 mmHg to 70 mmHg).

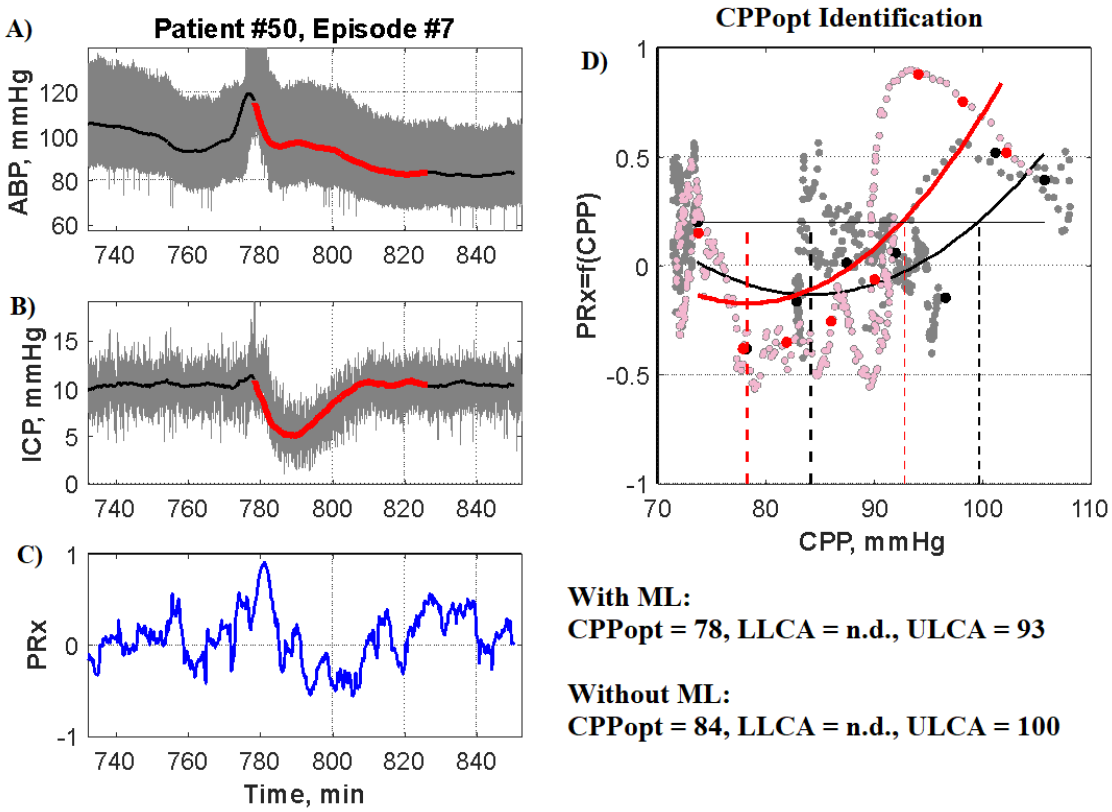

Fig. 22. Patient 50, Episode 7

Patient 50's episode 7 of 2-hour monitoring window after the application of the developed ML algorithm. A) and B) illustrate which episode out of the 2-hour monitoring window was selected as informative data by the developed ML algorithm, graphed in ABP and ICP, respectively. C) presents the calculated PRx value at each time using the associated values from ABP and ICP graphs over the entire 2-hour time window. D) presents the graph of CPP vs PRx. The patient's individual CPPopt range approximations according to ML are illustrated by the red line (CPPopt = 78 mmHg, LLCA = n.d., and ULCA = 93 mmHg), while values without ML are illustrated by the black line (CPPopt = 84 mmHg, LLCA = n.d., and ULCA = 100 mmHg). In this example, the application of ML has reduced the CPPopt value (from 84 mmHg to 78 mmHg) and lowered the ULCA value (from 100 mmHg to 93 mmHg).

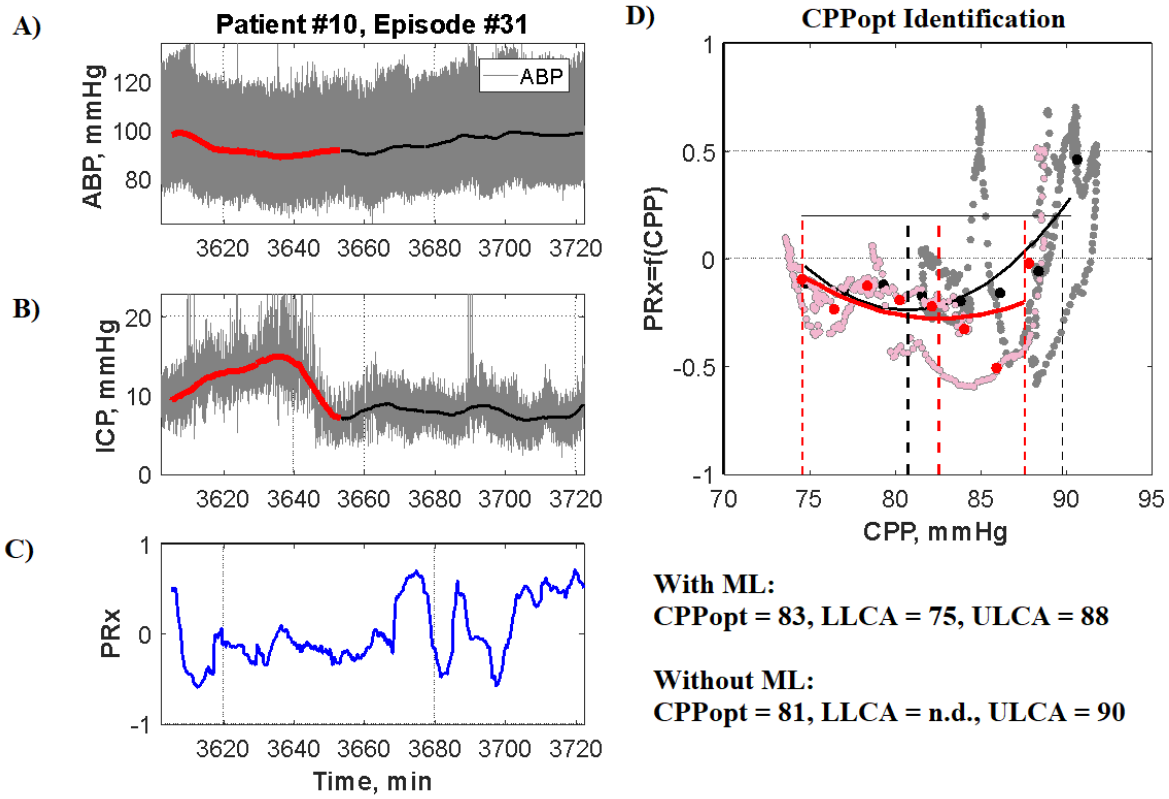

Fig. 23. Patient 10, Episode 31

Patient 10's episode 31 of the 2-hour monitoring window after the application of the developed ML algorithm. A) and B) illustrate which episode out of the 2-hour monitoring window was selected as informative data by the developed ML algorithm, graphed in ABP and ICP, respectively. C) presents the calculated PRx value at each time using the associated values from the ABP and ICP graphs over the entire 2-hour time window. D) presents the graph of CPP vs PRx. The patient's individual CPPopt range approximations according to ML are illustrated by the red line (CPPopt = 83 mmHg, LLCA = 75 mmHg, and ULCA = 88 mmHg), while values without ML are illustrated by the black line (CPPopt = 81 mmHg, LLCA = n.d., and ULCA = 90 mmHg). In this example, the application of ML has identified the individual's LLCA (75 mmHg), where it was unidentifiable prior to the use of ML.

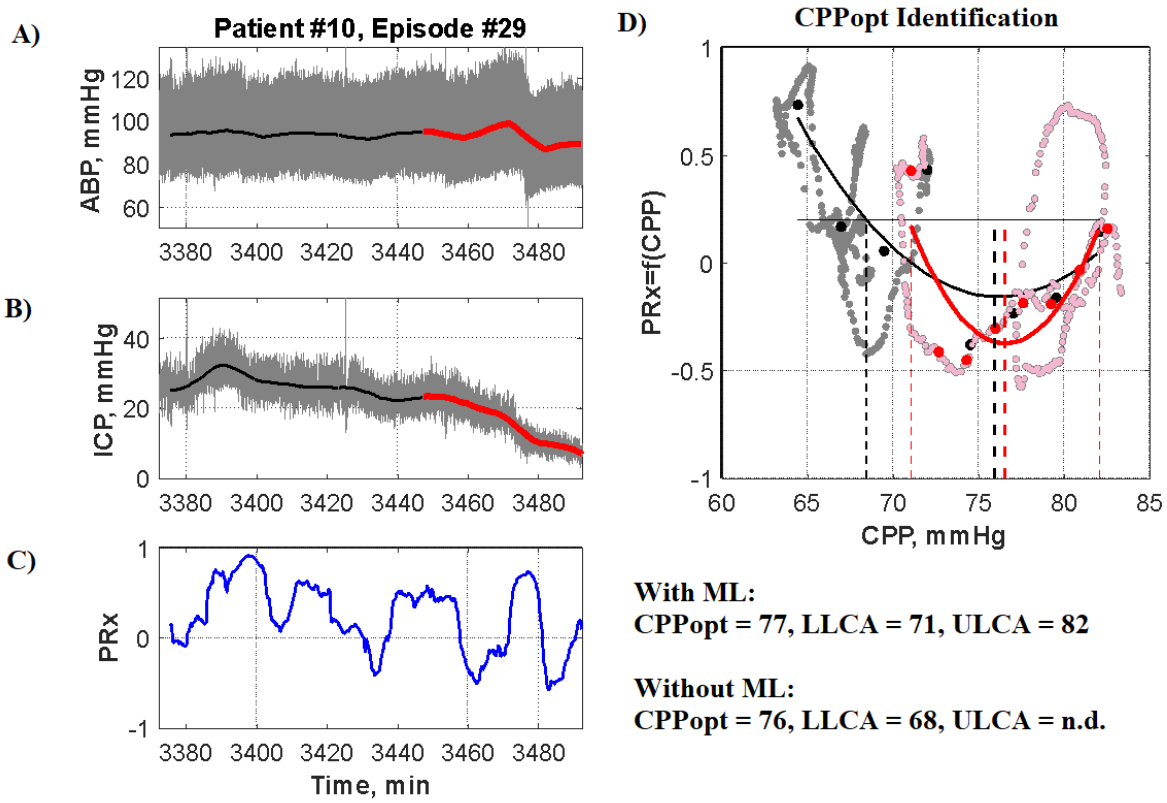

Fig. 24. Patient 10, Episode 29

Patient 10's episode 29 of the 2-hour monitoring window after the application of the developed ML algorithm. A) and B) illustrate which episode out of the 2-hour monitoring window was selected as informative data by the developed ML algorithm, graphed in ABP and ICP, respectively. C) presents the calculated PRx value at each time using the associated values from the ABP and ICP graphs over the entire 2-hour time window. D) presents the graph of CPP vs PRx. The patient's individual CPPopt range approximations according to ML are illustrated by the red line (CPPopt = 77 mmHg, LLCA = 71 mmHg, and ULCA = 82 mmHg), while values without ML are illustrated by the black line (CPPopt = 76 mmHg, LLCA = 68 mmHg, and ULCA = n.d.). In this example, the application of ML has identified the individual's ULCA (82 mmHg), where it was unidentifiable without ML.